

Serveur Académique Lausannois SERVAL serval.unil.ch

Author Manuscript

Faculty of Biology and Medicine Publication

This paper has been peer-reviewed but does not include the final publisher proof-corrections or journal pagination.

Published in final edited form as:

Title: Targeting of Fn14 Prevents Cancer-Induced Cachexia and Prolongs Survival.

Authors: Johnston A.J., Murphy K.T., Jenkinson L., Laine D., Emmrich K., Faou P., Weston R., Jayatilleke K.M., Schloegel J., Talbo G. et al.,

Journal: Cell

Year: 2015

Volume: 162(6)

Pages: 1365-1378

DOI: [10.1016/j.cell.2015.08.031](https://doi.org/10.1016/j.cell.2015.08.031)

In the absence of a copyright statement, users should assume that standard copyright protection applies, unless the article contains an explicit statement to the contrary. In case of doubt, contact the journal publisher to verify the copyright status of an article.

Targeting of Fn14 prevents cachexia

Amelia J. Johnston¹, Kate T. Murphy⁴, Laura Jenkinson¹, David Laine¹, Kerstin Emmrich¹, Pierre Faou¹, Ross Weston¹, Krishnath M Jayatilleke¹, Jessie Schloegel¹, Gert Talbo¹, Joanne L. Casey¹, Vita Levina¹, W. Wei-Lynn Wong¹, Helen Dillon¹, Tushar Sahay¹, Joan Hoogenraad¹, Holly Anderton¹, Cathrine Hall², Pascal Schneider⁵, Michael Foley¹, Andrew M. Scott⁶, Paul Gregorevic^{7,8}, Spring Yingchun Liu⁹, Linda C. Burkly¹⁰, Gordon S. Lynch⁴, *John Silke^{1,2,3} & *Nicholas J. Hoogenraad¹

¹Department of Biochemistry, La Trobe University, Kingsbury Drive, Melbourne, VIC 3086, Australia

²The Walter and Eliza Hall Institute, Melbourne, Australia

³Department of Medical Biology, The University of Melbourne, Melbourne, Australia

⁴Basic and Clinical Myology Laboratory, Department of Physiology, The University of Melbourne, Melbourne, Australia

⁵Department of Biochemistry, University of Lausanne, Epalinges, Switzerland

⁶Olivia Newton-John Cancer Research Institute, and La Trobe University, Melbourne, Australia

⁷Baker IDI Heart and Diabetes Institute, Melbourne, Australia, VIC, 3004

⁸Department of Biochemistry and Molecular Biology, Monash University, Clayton, VIC 3800, Australia.

⁹Broad Institute, MIT and Harvard, Cambridge, MA 02142, United States

¹⁰Department of Immunology, Biogen Idec, 14 Cambridge Center, Cambridge, MA 02142, United States

***Correspondence to silke@wehi.edu.au and N.Hoogenraad@latrobe.edu.au**

Summary

The cytokine TWEAK and its cognate receptor Fn14 are members of the TNF/TNFR Superfamily and are upregulated in tumors. We found that Fn14, when expressed in tumors, causes cachexia, and that antibodies against Fn14 dramatically extended lifespan by inhibiting tumor-induced weight loss while having only moderate inhibitory effects on tumor growth. Anti-Fn14 antibodies prevented tumor-induced inflammation and loss of fat and muscle mass. Fn14 signaling in the tumor, rather than in the environment, is responsible for inducing this cachexia because tumors in Fn14- and TWEAK-deficient hosts developed cachexia that was comparable to that of wildtype mice. These results

extend the role of Fn14 in wound repair and muscle development to involvement in the aetiology of cachexia and indicate that Fn14 antibodies may be a promising approach to treat cachexia, thereby extending lifespan and improving quality of life for cancer patients.

Introduction

TWEAK (Tumor Necrosis Factor TNF Superfamily member 12) and its cognate receptor Fn14 (TNFRSF12A) have been shown to play multiple roles in the process of wound repair and can promote angiogenesis, proliferation, migration, apoptosis and inflammation (Burkly et al., 2011; Campbell et al., 2004; Vince and Silke, 2006a; Winkles, 2008). Consistent with such a role, Fn14 expression is strongly increased following wounding (Wiley et al., 2001). It has been suggested that tumors resemble "wounds that do not heal" (Dvorak, 1986) and in line with this, Fn14 expression is also increased in solid tumors (Culp et al., 2010; Wiley et al., 2001). TWEAK/Fn14 signaling therefore contributes to carcinogenesis and targeting this pathway with monoclonal antibodies can inhibit tumor growth (Culp et al., 2010; Winkles, 2008).

TWEAK activates both canonical and non-canonical NF- κ B signaling pathways (Salzmann et al., 2013; Varfolomeev et al., 2007; Varfolomeev et al., 2012; Vince et al., 2008a), increases expression of genes associated with inflammation and fibrosis in myotubes (Panguluri et al., 2010) and promotes myofiber atrophy. *In vivo* studies using TWEAK transgenic and TWEAK or Fn14 knock-out mice support the idea that regulating myogenesis and muscle repair are physiological functions of the TWEAK/Fn14 signaling axis (Tajrishi et al., 2014). For example, transgenic overexpression of TWEAK in skeletal muscle leads to muscle atrophy in mice (Mittal et al., 2010a; Mittal et al., 2010b) while TWEAK-deficient mice have improved regeneration of skeletal muscle after injury (Girgenrath et al., 2006; Mittal et al., 2010a; Mittal et al., 2010b).

Cachexia is a complex disease, best described as a metabolic disorder that includes progressive muscle wasting with or without the loss of fat stores. It frequently presents in the terminal stages of many chronic illnesses including cancer (Tisdale, 2010). Cachexia may be present in 50-80% of patients with solid tumors (Dewys et al. 1980; Laviano et al., 2005; Walsh et al. 2000). Although cachexia reduces patient survival and response to chemotherapy, and may account for ~25% of all cancer deaths (Warren, 1932), the molecular mechanisms are still poorly understood and there are currently no FDA approved drugs for cachexia. Attempts to cure cachexia by increasing appetite or nutrition have so far proven unsuccessful in clinical trials. However, it has been suggested that interventions for cachexia could potentially be developed by targeting inflammatory processes that occur in concert with the wasting and metabolic imbalance that characterises the cachectic diagnosis (Muscaritoli et al., 2010).

Inflammatory cytokines that have been suggested to play a role in cachexia include TNF, Interleukin-1 (IL-1), IL-6 and Interferon- γ (Argilés et al., 2009; Ohnuma and Holland, 2009; Tisdale, 2009). Glucocorticoids may also contribute to cachexia by upregulating tumor-derived factors such as lipid-mobilizing

factor, which activates degradative pathways in adipose tissue leading to the breakdown of fat deposits and disrupted metabolic processes (Islam-Ali and Tisdale, 2001; McDevitt et al., 1995; Russell and Tisdale, 2005). Most recently, it has been shown that activation of the activin type-2 receptor ActRIIb (Zhou et al., 2010) by TGF- β family ligands drives a cachectic phenotype in mice and the degradation of myofibrillar proteins through the ubiquitin-proteasome pathway. Excitingly, given the dearth of pharmacological targets for this devastating disease, recombinant decoy ActRIIb inhibited activation of this pathway and significantly increased survival and muscle mass of mice bearing cachexia-inducing tumors (Zhou et al., 2010). Unfortunately decoy ActRIIb clinical trials in healthy adults and boys with Duchenne muscular dystrophy were stopped because of treatment-related bleeding issues and so have not been pursued for cachexia treatment. A modified version that has reduced Activin binding has however showed encouraging activity in promoting hematopoiesis in mice (Suragani et al., 2014).

Because of the demonstrated involvement of TWEAK/Fn14 signaling in tumor progression, we hypothesised that an antagonistic monoclonal antibody targeting Fn14 would inhibit tumor growth (Vince and Silke, 2006; Winkles, 2008). We therefore developed and characterized three antagonist monoclonal antibodies against Fn14. Two of these antibodies showed variable ability to block tumor growth but were strikingly effective at preventing tumor-induced weight loss. We demonstrated that the tumor-induced loss of lean and fat mass is consistent with the development of cachexia and that our Fn14 antibodies were able to prevent and reverse tumor-induced cachexia in different tumor models. Our results support the hypothesis that inhibiting Fn14 signaling has therapeutic potential for cancer-induced cachexia.

Results

Monoclonal antibodies against Fn14

To test the hypothesis that inhibition of Fn14 would limit tumor growth, we generated several antagonist monoclonal antibodies against Fn14 by inoculating wild type mice with recombinant human Fn14-Fc and generated hybridomas as previously described (Galfré and Milstein, 1981). The antibodies were positive when screened against a Mouse Embryonic Fibroblast (MEF) cell line stably expressing an inducible human Fn14 construct using flow cytometry. Three of these: 001, 002 and 004 are described here (Figure 1A). A commercially available anti-human Fn14, ITEM1 (Nakayama et al., 2003), also reacted with human Fn14 in a similar fashion (Figure 1A). ITEM1 and our three novel antibodies detected human Fn14 specifically by Western blot (Figure 1B). Human and mouse Fn14 are 92% identical in the extracellular domain, and consistent with this, two of the antibodies, 001 and 002 reacted against the uninduced MEF cell lines that express endogenous murine Fn14 (Figure 1A). Thus all of the antibodies specifically recognise human Fn14 and 001 and 002 also cross-react with murine Fn14.

Because members of the TNF Receptor Superfamily (TNFRSF) share some homology in their extra-cellular domain, if any proteins are cross reactive with our antibodies, members of the superfamily are the most likely candidates.

However many of these receptors are only expressed in specific hematopoietic lineages making it difficult to definitively rule out cross reactivity by screening cell lines. Therefore, a number of VSV- or HA-tagged TNFRSF members were over-expressed in HEK293T cells and reacted with either a VSV, HA, 001 or 002 antibody. All TNFRSF receptors were expressed and readily detected by the VSV or HA antibody, however only Fn14 was detected by 001 and 002 antibodies (Figure 1C).

To address whether the Fn14 antibodies activated or blocked Fn14-dependent signaling, we used a HEK293T cell line, that expresses endogenous human Fn14, stably transduced with a lentiviral NF- κ B reporter vector (Vince et al., 2008b; Figure 1D). The antibodies were unable to stimulate NF- κ B, demonstrating that in this assay they are not Fn14 agonists (left column, Figure 1D). Our antibodies, but not a control IgG antibody, did however block TWEAK/hFn14 induced NF- κ B (Figure 1D). To functionally assess the ability of our antibodies to inhibit TWEAK/hFn14 signaling we used human rhabdomyosarcoma Kym1 cells that are exquisitely sensitive to cell death induced by TWEAK (Schneider et al., 1999; Vince et al., 2008a). We co-cubated Kym1 cells with or without TWEAK (at 5, 50 or 200 ng/ml) and monoclonal antibodies at a concentration of 1 μ g/ml for 24 hours. All adherent and floating cells were harvested and stained with Propidium Iodide (PI) and the percentage of dead, PI-positive cells was determined by flow cytometry. Both antibodies 001 and 002 were able to inhibit TWEAK-induced death of Kym1 cells, however antibody 004 was ineffective in this assay (Figure 1E).

To define the epitope that the antibodies bound to, the structure of the extracellular domain of Fn14 was assessed (Pellegrini et al., 2013; Brown et al., 2006) and two ‘subdomains’ were generated as peptides. Antibody binding to these sub-domains was assessed by quantitative ELISA. All antibodies bound efficiently and specifically to sub-domain 2 but not to sub-domain 1 (Figure 1F and S1A). A series of point mutants of extracellular domain constructs representing human Fn14 and mouse Fn14 were generated for expression and purification from *E. coli*. These mutations were chosen based on mouse-human differences and also residues described to be important for binding of other known Fn14 antibodies. Consistent with the results from the other assays, 001 and 002 bound human and mouse Fn14 extracellular domains equally well, while ITEM1 bound better to human Fn14 than to mouse (Figure S1B). Furthermore, 001 and 002 bound point mutants of human Fn14 identically while ITEM1 and 004 had a distinct epitope binding profile (Figure S1B, D, E & F). In summary, these results demonstrate that 001 and 002 antibodies bound specifically to a defined extracellular epitope on the Fn14 receptor and can inhibit Fn14/TWEAK signaling. Antibody 001 is an IgG2b and 002 is an IgG1. Both recognize human and murine Fn14 and efficiently inhibit Fn14 signaling.

Fn14 antibodies increase survival of Colon-26 tumor-bearing mice

To test our hypothesis that an antagonistic Fn14 antibody could inhibit tumor growth we used the Lewis Lung Carcinoma (LLC) and Colon-26 (C-26) tumor cell lines commonly used in allograft studies that respectively express low and high Fn14 levels (Figure 2A). In the C-26 tumor model, groups of five immunocompetent CD2F1 mice were inoculated with 1×10^6 C-26 tumor cells,

then treated or not with the 002 antibody on days 5, 12, 15 and 20 post-inoculation. Tumor growth displayed some inter-individual heterogeneity, but growth was on average slightly slower in the treated compared to the untreated mice (Figure 2B). However the survival of the treated mice was dramatically extended (Figure 2C). While the tumors in untreated and treated animals were comparable in size over the 18 days post inoculation, untreated mice lost weight rapidly from day 11 onwards while treated mice maintained weight and condition during this period (Figure 2D). Maintenance of weight in a pair fed control group showed that the decrease in body mass in the untreated C-26 tumor mice was not due to differences in food intake (Figure 2D).

Fn14 antibodies block Colon-26 tumor-induced cachexia

Both the LLC and C-26 cell lines have been shown to induce cachexia in mice, although the LLC model is generally milder in disease severity (Murphy et al., 2012; Zhou et al., 2010). Hallmarks of this disease include loss of lean body mass, loss of muscle function and systemic inflammation (Murphy et al., 2012). This is in stark contrast to starvation where lean body mass and muscle function are preserved in the short term. To test whether the anti-Fn14 antibody inhibited cachexia in C-26 tumor bearing mice, we treated 10 mice with either anti-Fn14 or an isotype control IgG (IgG1) dosed on days 8, 12 and 16 post tumor inoculation and sacrificed them at day 22. For pragmatic reasons these experiments were performed in different labs with a different source of C-26 tumor cell line. As observed before in the absence of therapy, C-26 tumor mice began to lose weight around 11 days post tumor inoculation, and although there was a slightly slower decline in weight using this alternative source of C-26 cells, anti-Fn14-treated mice retained body weight (Figure 3A). In a separate experiment, untreated C-26 tumor bearing mice were compared to a non-tumor “PBS” group that were injected with PBS in place of C-26 cells and then paired against the C-26 group (blue and grey lines, respectively). On comparison, the anti-Fn14 treated mice actually had higher relative body mass than the paired PBS controls by the end of the experiment (Figure 3A). As before, tumors in the antibody-treated mice grew slower than in control mice but weight loss was already well advanced by day 17 when tumor size differences were negligible, indicating that the anti-tumor effect of the antibody was not the reason for the reduction in cachexia (Figure S2, Figure 3A). The preservation of weight in the anti-Fn14-treated mice was even more apparent when the weights of the mice without tumors were measured (Figure 3B). Furthermore, the mass of several muscles (soleus, extensor digitorum longus [EDL], plantaris, tibialis anterior [TA], gastrocnemius and quadriceps) in anti-Fn14-treated mice was significantly spared compared to the untreated and control IgG-treated mice such that muscle mass was similar to PBS controls (Figure 3C, D). Heart mass was also significantly spared in anti-Fn14-treated mice and similar to non-tumor-bearing, PBS-injected control (Figure 3D). Not only did anti-Fn14 treatment prevent loss of epididymal fat mass in C-26 tumor-bearing mice compared to control-treated and untreated mice but fat mass was even increased above controls with no tumors (Figure 3E). Consistent with the preservation of muscle mass, peak grip strength in living mice at day 21 was increased in anti-Fn14-treated mice compared to untreated and control IgG treated mice (Figure 3F). Peak twitch force (Figure 3G), peak tetanic force (Figure 3H) and tetanic force over a range of stimulation frequencies (Figure 3I) of TA muscles assessed *in situ* was also

significantly higher in anti-Fn14-treated animals compared to untreated and control-treated mice, and reached forces similar to those obtained in non-tumor controls. After determining peak tetanic force, muscles were subjected to a four minute intermittent stimulation protocol to induce muscle fatigue. Again, the TA muscles of anti-Fn14-treated mice produced higher forces throughout most of the fatiguing stimulation protocol than the control and untreated mice (Figure 3J).

These results strongly suggested that C-26 tumor mice treated with anti-Fn14 antibody were resistant to cachexia. To investigate this observation at the cellular level, TA muscle sections were stained with hematoxylin and eosin (H&E), revealing a larger fiber size in anti-Fn14-treated mice compared with the untreated and control treated mice and similar to PBS controls (Figure 4A). Sections stained with anti-laminin confirmed the increase in muscle fiber size in anti-Fn14-treated mice (Figure 4B), and co-staining with a myosin IIa specific antibody (N2.261) to identify type IIa and type IIx/b fibers (non-N2.261 reacting fibers) revealed that the cross-sectional area of both fast, oxidative type IIa fibers and fast, glycolytic type IIx/b fibers was increased with anti-Fn14 (Figure 4C, D). The proportion of type IIa and type IIx/b fibers was similar between treated and untreated groups (Figure 4D), as was muscle fiber oxidative capacity as assessed by reacting for succinate dehydrogenase activity (SDH, Figure 4C, E). These results show that the protection of muscle mass and strength with anti-Fn14 treatment was due to the protection of individual muscle fibers and not a shift in muscle fiber type composition.

TWEAK signaling has been shown to induce muscle atrophy through activation of the ubiquitin proteasome and inhibition of the Akt/p70S6K pathway (Dogra et al., 2007). We therefore investigated the effect of anti-Fn14 treatment on the mRNA expression of the ubiquitin ligases MuRF-1 and atrogin-1. Consistent with the increase in muscle mass and fiber size in anti-Fn14-treated mice, MuRF-1 and atrogin-1 mRNA expression was significantly reduced in the TA muscle of anti-Fn14-treated tumor-bearing mice compared with untreated and IgG-treated mice and the levels in the non-tumor-bearing mice (Figure 4F). In addition to the loss of muscle, mRNA expression of the inflammatory cytokines IL-6 and TNF were significantly higher in TA muscles from C-26 control and IgG-treated mice compared to anti-Fn14-treated mice, indicating that anti-Fn14 protects mice from muscle loss and also reduces the cachectic inflammatory phenotype (Figure 4G).

To test whether anti-Fn14 antibody inhibited cachexia in mildly cachectic LLC tumor-bearing mice, we treated mice with either anti-Fn14 (002) or an isotype control IgG dosed on days 7, 14, 21 and 28 post tumor inoculation and sacrificed them at day 35. Antibody treatment slowed tumor growth (Figure S3A, B) and although it had no significant effect on body mass in the PBS groups (Figure S3C), it slightly increased body mass in LLC tumor-bearing mice (Figure S3D).

Fn14-expressing tumors cause severe cachexia in mice

Collectively, results obtained with anti-Fn14 antibody 002 suggested that Fn14 signaling was sufficient to promote cancer-induced cachexia. To test this hypothesis, fibroblast cell lines derived from C57BL/6 embryos and transformed

with a H-Ras V12 oncogene were infected with a hFn14-expressing lentivirus. As a control, we infected the same parental cell line with a lentivirus expressing only the extracellular domain of hFn14 fused to a GPI anchor. Both hFn14 and control cell lines formed tumors when injected into mice and initially grew at similar rates (Figure 5A). Eight days post inoculation, mice bearing hFn14 expressing tumors, but not the control tumors, suffered rapid weight loss and their overall health deteriorated quickly (Figure 5B). Post mortem analysis of these mice revealed increased vasculature (Figure 5C) and tumor invasive capacity (Figure 5D) in the hFn14-expressing tumors when compared with controls.

Fn14 antibodies block Fn14-induced cachexia in mice

As further confirmation of our hypothesis that blocking Fn14 signaling prevents cachexia we used the monoclonal 001 in the following experiments. Antibody 001 has an Fn14 binding profile and ability to block Fn14 signaling that is almost identical to antibody 002 but has some differences (total of 15 amino acid differences across the 6 CDR regions in the heavy and light chain sequences and is a different isotype [IgG2b]). Mice were inoculated with MEF tumor cells expressing Fn14 or not and on the first day of marked weight loss (day 6) were treated with antibody 001 or IgG2b isotype control. The experiment was run for 11 days when a clear decline in weight and condition was seen in the IgG2b-treated controls. As before, hFn14 expressing tumors caused a loss of body mass (Figure 6A), and a single treatment with anti-human Fn14, but not the isotype control antibody, substantially prevented this loss (Figure 6A-C), even though tumor mass and volume was not significantly different between groups (Figure S4). Fn14 tumors caused a significant decrease in mass of the TA and plantaris muscles and a trend for lower muscle mass of EDL, soleus, gastrocnemius and quadriceps ($P < 0.09$, Figure 6C). There was no significant change in heart mass in Fn14 tumor bearing mice (Figure 6D) but a significant decrease in subscapular fat mass (Figure 6E). Remarkably, the loss of muscle and fat mass in hFn14-expressing tumor mice was reduced by a single injection of anti-human Fn14 antibody (Figure 6C & E).

The contractile properties of muscles in live mice were assessed on day 11 but there were no significant differences between groups in grip strength (data not shown), and in anesthetized mice there were no differences in peak twitch force (data not shown), peak tetanic force and specific (normalized) force of TA muscles *in situ* (Figure 6F). However, tetanic force over a range of stimulation frequencies (10-300 Hz) was lower in TA muscles from mice with hFn14 tumors than mice bearing control tumors and this reduction in force was prevented by treatment with anti-Fn14 (Figure 6F, left panel). Anti-Fn14 also increased relative force production during and after a 4-minute intermittent fatiguing stimulation protocol, indicating reduced muscle fatigability following anti-human Fn14 treatment (Figure 6G).

TA muscle sections were stained with H&E, anti-laminin, and anti-myosin IIa (N2.261) antibodies to examine the effect of Fn14 tumor expression on muscle fiber architecture and fiber cross-sectional area (Figure 6H). Consistent with the C-26 experiments, hFn14 tumors caused a significant decrease in muscle fiber cross-sectional area (Figure 6I), which was due to decreases in size of both type

Ia and type Iix/b fibers (Figure 6J). Remarkably, a single injection of anti-Fn14 prevented the decrease in muscle fiber size (Figure 6H & I). It was also interesting to note the greater space between individual fibres in hFn14 tumor-bearing mice that was absent after anti-Fn14 treatment (Figure 6H). Despite improvements in muscle fatigability, anti-Fn14 did not cause a shift in fiber type proportions (Figure 6H & J) or muscle fiber oxidative capacity as assessed by SDH reaction intensity (Figure 6H & J). Assessment of mRNA levels of IL-6, an inflammatory marker of cachexia in TA muscle, also revealed that similar to the C-26 tumor-bearing mice, hFn14 tumors caused a significant increase in IL-6 expression in TA muscles compared to control tumors and anti-Fn14 treatment blocked this increase (Figure 6K).

Not all Fn14 antibodies are anti-cachectic

Given the success of two different Fn14 antibodies (001 and 002) in blocking weight loss and extending survival in tumor-bearing mice, we asked whether any Fn14 antibody would be efficacious against the symptoms of cachexia. We therefore assessed our third antagonistic antibody, 004, along with a commercially available antibody, ITEM1. 004 is specific to human Fn14 and unlike either 001 or 002 did not cross react with murine Fn14. ITEM1, unlike either 001, 002 or 004, did not antagonise TWEAK/Fn14 signaling in the NF- κ B reporter assay (Figure 1D, Figure S5). Human Fn14 expressing MEF tumors were established in mice and a single dose of antibody was administered at day 7, just prior to noticeable weight loss, to randomized groups of mice. Consistent with the preceding experiments, 001 and 002 prevented weight loss induced by Fn14 tumors (Figure 7A) and improved survival (Figure 7B) yet all groups of mice had similar tumor sizes over the critical differential survival period (Figure 7C). However 004 and ITEM1 were unable to prevent Fn14 tumor-induced weight loss or improve survival. These observations were also confirmed in an independent study where antibody was administered after the onset of weight loss (Figure S6). These results suggest that neither the ability to bind human Fn14 nor antagonistic properties of an antibody to human Fn14 are sufficient to predict its ability to inhibit cachexia.

Host TWEAK and Fn14 are not involved in propagating cachexia

TWEAK/Fn14 signalling has been reported to play a role in muscle atrophy (Tajrishi et al., 2014). To determine whether tumors were a direct or indirect source of TWEAK and thereby promoted Fn14-dependent muscle loss, we established Fn14 tumors in *Fn14*⁻ and *Tweak*-deficient mice. Mice were inoculated with MEF Fn14 tumor cells on day 1 and body weight and tumor size were monitored (Figure 8). Body, tumor, muscle (TA, Quad, heart) and epididymal fat weight (male mice) were assessed (Figure 8A, B & C). There were no differences in the onset, severity or timing of cachexia in either strain of knock-out mice suggesting that neither host (muscle or other tissue) Fn14 nor TWEAK play a causative role in the muscle atrophy or fat loss induced by this tumor. The starting weights are standardised for ease of visualisation of the data, but the average starting weights of wild type (29.7g), *Fn14*⁻ (28.5g) and *Tweak*⁻ (26.4g) mice were approximately equivalent.

The monoclonal anti-TWEAK antibody MTW-1 has been shown to be effective in reducing collagen induced arthritis and blocking macrophages from

infiltrating tumors *in vivo* (Kaduka et al., 2005; Kamata et al., 2006). *In vitro*, MTW-1, but not an isotype control antibody, blocked TWEAK induced NF- κ B in our reporter assay (Figure 8D). To test the ability of MTW-1 to prevent MEF Fn14-induced cachexia, wildtype mice with tumors were treated with this antibody or an isotype control antibody (Rat IgG) on day 7 and body weight was monitored over time. In contrast to the anti-Fn14 antibody treatment, MTW-1 (anti-TWEAK) had no effect on the rapid induction of cachexia by the MEF Fn14 tumor (Figure 8E). Together these results show that neither tumoral nor humoral sources of TWEAK drive cachexia in this model.

Using a next generation sequence approach to survey gene expression, we recently found that muscle wasting induced by local transduction of mouse limb muscles with a recombinant adeno-associated virus based vector expressing activin A (AAV:ActA) was associated with up-regulation of Fn14 transcription (Chen et al., 2014). Abundance of Fn14 protein, as determined by Western blot, was increased approximately 10-fold in muscles administered the activin-expressing vector, compared with contralateral limb muscles administered a control vector (Chen et al., 2014). Because local over-expression of activin A induced marked muscle wasting, we asked whether induction of Fn14 was causative of muscle wasting in activin A over expressing muscle. To test this, we transduced the right tibialis anterior hind-limb muscles of C57BL/6 mice with our aforementioned AAV vector expressing activin A, and administered a control AAV vector in the left TA muscle. Mice were treated with antibody 001, 002 or an IgG control antibody commencing four days after administration of AAV vectors, and for a total of six injections per mouse prior to assessment at the experimental endpoint four weeks after vector administration. As we previously reported, increased local expression of activin A caused muscle wasting (Figure 8F, G), however, neither the 001 nor 002 Fn14 antibodies blocked activin A-induced muscle loss. These results indicate that while Fn14 is up-regulated in muscle during activin A-induced muscle wasting, it is not causative of the observed loss of muscle mass.

Given the dramatic procachectic effects of Fn14-expressing tumors in mice, it was of interest to see if there is any correlative data that might indicate whether the same scenario pertains in human cancers. We examined the mRNA expression and clinical data for a range of cancers in the GDAC (Genome Data Analysis Centre) Firehose at the Broad Institute (<https://confluence.broadinstitute.org/dosplay/GDAC/home>). For cancers where sufficient sample sizes exist, there is a positive correlation for the expression of Fn14 with proinflammatory cytokines in human cancers (Figure S7). In breast, head and neck, lung, colorectal and stomach cancer, IL-1 α (Figure S7A), IL-1 β (Figure S7B), IL-6 (Figure S7C), IL-8 (Figure S7D) and TNF (Figure S7E) all correlate positively with Fn14 expression. Correlation coefficients that are statistically significant at Benjamini and Hochberg adjusted P-value <0.05 are highlighted (*; Benjamini, 1995) and underscore that for the largest sample sizes (Breast and Lung) there is a strong statistical correlation between Fn14 and inflammatory cytokine expression by the tumors (Figure S7F).

Discussion

We developed antibodies to Fn14 to specifically block Fn14 signaling in order to reduce tumor growth and development. Our antibodies were specific and were selected on the basis that they inhibited TWEAK-Fn14 induced NF- κ B signaling and cell death. We initiated studies *in vivo* thinking therefore that these antagonistic antibodies might impede tumor growth (Wiley et al., 2001; Winkles, 2008; Lassen et al., 2015; Yin et al., 2013). Our antibodies however had incomplete and tumor specific effects on tumor growth; LLC tumor growth was inhibited most whereas Ras transformed MEF tumor growth was affected very little.

In the C-26 model there was an intermediate effect on tumor growth of our antibodies however the most remarkable effect of the antibodies was to dramatically prevent loss of weight, ameliorate the general condition and prolong survival. Tumors can cause anorexia, or suppress appetite (Maccio et al., 2012), however in this case loss of weight was not due to a tumor effect on feeding because pair fed controls retained body mass.

Cachexia is a poorly understood disease and a co-morbidity with many conditions of chronic illness in addition to cancer. The defining hallmark of cachexia is loss of lean muscle mass and in some cases loss of fat. Our poor understanding of the signaling pathways causing cachexia has meant that current cachexia therapies generally target the symptoms rather than the cause of the disease. For example, Ghrelin, a peptide hormone originally isolated from the stomach that stimulates appetite, has been used in cachectic patients to combat loss of body mass (Maccio et al., 2012). However while clinical trials with Ghrelin show some promise it is ultimately ineffective because it does not address the cause of the disease.

We therefore investigated the possibility that TWEAK/Fn14 signaling might contribute to cachexia. In our experiments, untreated and control-treated tumor-bearing mice lost significant muscle mass from all of the major skeletal muscles and this loss was prevented by treatment with anti-Fn14. Furthermore, muscle function was also retained in the antibody-treated mice, along with fat stores and a decrease in inflammatory markers within target tissue was also observed.

We had specifically chosen antibodies to Fn14 that are able to antagonize the action of TWEAK, in line with the hypothesis that Fn14-dependant cachexia is caused by an activation of signaling through Fn14. Although *in vitro* our antibodies could function as antagonists, a question that remains to be tested is whether they act as antagonists *in vivo*. We cannot rule out that *in vivo* these anti-cachectic antibodies are operating via Fc dependant multimerisation pathways and *in vitro* studies have shown the potential of cross-linked Fc domains to reveal agonistic activity (data not shown). This is a common and often desirable feature of antibodies and has been demonstrated for other Fn14 antibodies (Culp et al., 2010; Salzman et al., 2013).

In addition to its effects on angiogenesis, TWEAK/Fn14 signaling has been linked to inhibiting myoblast to muscle differentiation (Dogra et al., 2006;

Girgenrath et al., 2006) and promoting myoblast proliferation. While *Tweak* (*Tnfsf12*) and *Fn14* knock-out mice develop normally without any obvious difference in body or muscle mass, *Tweak* deficient mice lost less muscle mass following injury than wild type mice (Mittal et al., 2010a). This implies that TWEAK/Fn14 does not play a role in the normal development of muscle but may, in pathological scenarios, promote muscle loss directly. Consistent with this, TWEAK transgenic mice are smaller and have reduced muscle mass, reduced muscle fiber cross sectional area, and increased markers of ubiquitin proteasome activation (Dogra et al., 2007; Mittal et al., 2010a). Combined with the ability of our Fn14 antibody to inhibit cachexia, these observations naturally led to the hypothesis that TWEAK is the factor that drives muscle wasting in cancer induced cachexia. However the MEF tumors induced cachexia in both *Fn14*^{-/-} or *Tweak*^{-/-} mice which is inconsistent with this hypothesis. In addition to its effect on muscle, TWEAK has been shown to be required for liver regeneration following partial hepatectomy (Jakubowski et al., 2005; Karaca et al., 2014). Together these reports suggest that physiological levels of TWEAK contribute to regeneration of injured tissues, but that supraphysiological levels can promote damage, but that neither paradigm is relevant to cancer induced cachexia.

Consistent with this concept, we showed that cachectic mice treated with a TWEAK-blocking antibody still developed cachexia. These results argue against the possibility that tumor-derived TWEAK is the causative factor in cancer cachexia and raise the question of the nature of the soluble factor produced by the tumor. Potential candidates for such signaling molecules could be activins or myostatin because cachexia induced by C-26 tumors was prevented by a decoy activin receptor (ActRIIb) that inhibits activin/myostatin signalling (Zhou et al., 2010). Interestingly, although muscle wasting caused by C-26 tumors was successfully prevented by the ActRIIb decoy receptor, fat loss, another feature of cachexia, was unaffected (Zhou et al., 2010). In contrast anti-Fn14 treatment of C-26 cachectic animals prevented tumor induced inflammation, fat loss and reduction in muscle mass and function. Minimally we can conclude that if activin functions downstream of Fn14 to induce cachexia it is only one of the components produced by Fn14 tumors.

Intriguingly, activin A over expression in muscle promotes up regulation of Fn14 and muscle wasting, implying that Fn14 signalling works downstream of activin. However Fn14 antibodies did not prevent activin A-induced muscle loss. These results further support the idea that, physiologically, Fn14 is up-regulated as part of a protective reparative response in muscle rather than to promote muscle loss. In tumors, however, there is an elevated expression of and constant activation of Fn14 that leads to pathological consequences in peripheral tissues.

Phase I clinical trials using a soluble ActRIIb decoy receptor in Duchenne muscular dystrophy, begun in 2010, were terminated in 2011 because of increased incidence of nosebleeds, bleeding gums and dilated blood vessels in the skin. Because activin/myostatin play numerous roles throughout the body, it is, in hindsight, not surprising that blocking this pathway may lead to other side effects. Fn14 is therefore very attractive as a therapeutic target because it is not required for normal development. Its expression is strongly induced by growth

factors *in vivo* at sites of tissue injury, remodeling and in tumors (Culp et al., 2010; Feng et al., 2000; Winkles, 2008).

Cachexia in human cancer patients usually progresses slowly with an average loss of 5% body mass over 12 months, whereas cachectic mice lose weight very rapidly. In humans however, tumor mass as a proportion of body weight rarely exceeds 1%, while in murine tumor models the tumor can account for as much as 10% of the total mouse weight. Mice also have a different metabolism to humans. Despite the need to be cautious when translating results from mouse models to humans, it is noteworthy that in our experiments similar sized tumors caused very different cachectic effects. This demonstrates that cachexia is an active process with the tumor directly driving the loss of muscle and fat.

Our analysis of the TCGA database revealed positive correlations between many inflammatory cytokines implicated in cancer cachexia and Fn14 transcripts in patients. However this data cannot directly address whether Fn14 expression plays a role in cachexia because databases are not annotated for cachexia presence or the contribution of cachexia to patient survival. Even though the incidence of cachexia in cancer patients has been estimated to be as high as 80% depending on the definition used (Wallengren et al., 2013), current databases are remarkably deficient concerning this important contributor to patient well being and survival. Our results therefore indicate a pressing and urgent need to generate patient sample data that acknowledges and records this important component.

A therapy that directly targets cancer associated cachexia is desperately needed, because cachexia has been estimated to occur in a significant proportion of cancer patients before death and contributes to their inability to tolerate intensive treatment regimes (Argilés et al., 2009; Murphy and Lynch, 2009). Furthermore, cancer cachexia is associated with severe fatigue and systemic inflammation that directly affects quality of life, that may in turn negatively affect a patient's willingness to continue treatment (Maccio et al., 2012). The fact that anti-Fn14 reagents are already well tolerated by cancer patients in clinical trials (Lam et al., 2011) argues strongly that interventions that inhibit Fn14 should now be tested for their efficacy in cancer patients presenting with hallmarks of cachexia.

Materials and Methods

Monoclonal antibody generation - Immunisation of mice

Purified recombinant Fn14-Fc (“TWEAK receptor”, tandem repeat, Tetramer; obtained from Amgen) was used for immunisations. Female Balb/c mice were immunised IP with 15 µg of antigen in PBS emulsified in Complete Freund’s Adjuvant (Sigma) and incomplete Freund’s adjuvant (Sigma) for subsequent boosts. Boosts were performed at intervals of 4 weeks and a final intraperitoneal (IP) injection was given 3 days before spleens were removed and the spleen cells harvested. Test bleeds were taken 3-5 days post boost via the retro-orbital plexus and used for screening for the presence of an immune response. Blood collected from mice was allowed to clot at room temperature. The clot was removed by centrifugation and the serum collected and stored at -20°C.

Hybridoma production

Hybridoma fusions were performed using ClonaCell®-HY Hybridoma Kit (Stemcell Technologies) according to the manufacturer's instructions. Briefly, spleen cells were isolated by spleen perfusion before fusion with mouse myeloma SP20. The selection and cloning steps were performed on methylcellulose-based semi-solid media in 96 well plates. The culture supernatants were screened by ELISA for IgG production and subsequently by flow cytometry for specificity to Fn14.

Flow cytometry screening

1×10^5 MEF H-Ras V12 Fn14 +/- induced with 100 nM 4-hydroxytamoxifen (4OHT) were used as a single population prior to staining. Cells were incubated at 4°C with samples or controls for 30 min in PBS, 2% BSA. Cells were washed and incubated with secondary antibody (AlexaFluor-647-conjugated goat anti-mouse IgG, Invitrogen) for 30 min at 4°C in the dark. The BD FACSCanto II was used to perform flow cytometry according to the manufacturer's protocol and data analysis was performed using FlowJo. Experiments were representative of at least three independent experiments.

Purification of antibody

Approximately 2L of serum-free conditioned medium was collected per antibody over 5 days from 4 Triple Flasks 500cm² (Thermo Scientific) of hybridomas cultured in Hybridoma Serum Free Media (Invitrogen) supplemented with penicillin-streptomycin. Medium was filtered through a 0.45 µm filter prior to purification. Antibodies were purified by affinity chromatography with a 5 ml column of Protein A Sepharose HiTrap MabSelect Xtra (GE Healthcare). The Protein A column was equilibrated with buffer containing 0.02 M sodium phosphate, 250 mM NaCl pH 6.85 and the antibodies were eluted with 0.1 M Glycine/HCl pH 3.0, followed by neutralization with 1 M Tris/HCl pH 9.0. The neutralized eluate was concentrated and the buffer was exchanged with PBS using a vivaspin 20 column (Sartorius). Endotoxin was removed from samples using Detoxi-Gel (Thermo Scientific) and measured with E-toxate kits (Sigma) according to manufacturer’s instructions or using the Charles River Endosafe PTS Portable Test System. Endotoxin levels of all final antibody preparations used for *in vivo* experiments were determined to be below the level of detection of the assay (less than 0.05 EU/mg of antibody).

Antibody isotyping

Antibodies were isotyped using the BD Cytometric Bead Array (CBA) Mouse Immunoglobulin Isotyping Kit according to the manufacturers instructions.

Preparation of cell membranes for western blotting

MEF H-Ras V12 and MEF H-Ras V12 Fn14 cells were grown to around 50% confluency then induced for 48 h by the addition of 4-OHT (100 nM). Cells were harvested and washed with PBS, centrifuged and resuspended in 1 ml of 20 mM Tris, pH 7.4 with 10 µg/ml final concentrations of DNase1 and RNaseA. Cells were lysed and the genomic DNA sheared using a 27 G insulin syringe. Samples were centrifuged at 600 g at 4 °C for 3 min and the supernatant was collected and centrifuged at 20,000 g for 30 min at 4 °C. The pellet was resuspended in 80 µl of 1M Tris, 0.4% SDS. The final membrane preparations were stored at -20 °C. Proteins were separated on 4-12% Bis-Tris gel SDS PAGE. Western transfer to PVDF membrane was performed using a semi-dry apparatus. The PVDF filters were probed using antibodies 001 (1 µg/ml), 002 (1 µg/ml), 004 (10 µg/ml) and ITEM1 (Biolegend; 5 µg/ml). HRP-conjugated secondary goat anti mouse antibody was used for detection.

Flow cytometry of cell lines for Fn14 expression levels

Colon-26 (C-26) and Lewis Lung Carcinoma (LLC) cells adapted for growth in 0.5% fetal calf serum, were assessed for Fn14 expression levels. Cells were stained using commercially available anti-Fn14 antibody ITEM1 (5 µg/ml) and detected using an AlexaFluor-647 secondary antibody (10 µg/ml). Cells were resuspended in 1% BSA/PBS then assessed by flow cytometry on a BD FACS Canto II.

Cloning of Fn14 and Fn14-GPI constructs for tumor cell lines

The 4-hydroxytamoxifen (4OHT) inducible lentiviral infection system (Vince et al., 2007) was used. The full length wildtype cDNA for human Fn14 (NM_016639) was cloned into the lentiviral vector pF_UAS_Neo at *Bam*H I and *Nhe* I. The control construct containing the cDNA for the extracellular region of Fn14 (Forward CGCGGATCCATGGCTCGGGGCTCGCTGCGC Reverse GCTGGTGGTCATCCAAAGCAGCCGGAAGGGGGCAGG) fused to the TrailR3 GPI anchor coding region (AF020502) was created by overlap PCR (Forward primer CGGCTGCTTTGGATGACCACCAGCCCGGGGACTCCT, Reverse primer CGCGCTAGCTTATCAAACAAACACAATCAGAAG) to create Fn14-GPI. Constructs were confirmed by DNA sequencing.

MEF cell lines for in vivo tumor model (Fn14 and Fn14-GPI)

SV40 immortalised mouse embryonic fibroblasts (MEFs) from wildtype C57 Black 6 mice were transformed with human H-Ras V12 by retroviral infection. H-Ras V12 transformed cells were then infected with lentivirus for GEV16 and either Fn14 or Fn14-GPI. Cells were selected with appropriate antibiotics for a minimum of 2 weeks before flow cytometry screening was performed to confirm protein expression. The Fn14 expressing cell line was used in experiments described in Figure 5 or passaged once in mice prior to being used for all other experiments.

TNFRSF cross reactivity assessment

HEK 293T cells were transiently transfected with DNA constructs coding for various TNFRSF members using Lipofectamine 2000. The TNFRSF coding regions included an N-terminal VSV or HA tag. 24 hours post transfection, cells were harvested and lysed in RIPA buffer (150 mM NaCl, 0.1% SDS, 0.5% Sodium deoxycholate, 1% TritonX-100, 50 mM Tris-HCl pH 7.2) with added DNaseI (2 µg/ml), RNaseA (2 µg/ml) and protease inhibitors (Roche). Samples were prepared in SDS-PAGE sample buffer containing β-mercapotethanol and proteins were separated by SDS-PAGE and after western transfer the expression of TNFRSF members were detected using either an anti-VSV antibody or anti-HA. Membranes were also probed using 001 and 002 for antibody cross reactivity.

HEK293T NF-κB GFP assay

HEK293T cells containing a stably integrated NF-κB promoter followed by GFP open reading frame were used to test for functionally active antibodies (Vince et al., 2008a). Cells were incubated for 24 h in the presence or absence of purified recombinant Fc-TWEAK at a concentration of 50, 100 or 200 ng/ml. In addition, purified antibody (100 ng/ml or 1 µg/ml) or controls were added. Cells were harvested and GFP fluorescence was measured by flow cytometry (BD FACS Canto II, Diva software). A minimum of 10,000 events per sample were recorded. Isotype controls were used at equivalent concentrations. ITEM1, IgG2b, IgG1, Anti-TWEAK (MTW-1) and Rat IgG1 control antibody were purchased from Biolegend.

Kym1 cell death assay

Kym1 cell death assays were performed (Vince et al., 2008b) as described for the HEK293T NF-κB-GFP assay. Cells were incubated for 24 h in the presence or absence of Fc-TWEAK (5, 50 or 200 ng/ml), and purified antibodies (100 ng/ml or 1 µg/ml) or controls. Total cells were harvested and analysed by flow cytometry in the presence of Propidium Iodide (PI; Sigma P4170) at a concentration of 1 µg/ml. Data was graphed as the percentage of cell death.

Tumor cell lines and tumor studies

Cell lines used included two independent sources of Colon-26 cells (C-26; Cell Line Services; Germany and kindly donated by Martha Belury, The Ohio State University, Columbus, OH), Lewis lung carcinoma (LLC; European Collection of Cell Cultures). Cells cultured in 10% DMEM (MEF cell lines and LLC) or 10% RPMI (C-26) were grown to a confluency of 80% and then harvested using brief trypsinisation. Cells were centrifuged at 1,000 g for 7 min followed by 2 washes in phosphate buffered saline (PBS). Cell viability was assessed using trypan blue.

Mice were obtained from the Animal Resources Centre (Canning Vale, Western Australia) or Monash Animal Services (Monash, Victoria) and all experiments described throughout that involved the use of mice were approved by the Animal Ethics Committees of La Trobe University (AEC 13-52, 10-54, 11-37 & 10-19B), The University of Melbourne (AEC 1112069) and the Alfred Medical Research and Education Precinct (AEC E/1289/2012/B) and conducted in accordance with the *Australian code of practice for the care and use of animals*

for scientific purposes as stipulated by the National Health and Medical Research Council (Australia). Mice were housed under a 12:12-hour light-dark cycle. Mouse weights, the formation of solid tumors and general clinical health observations were taken daily throughout the duration of experiments. Tumor measurements were made using digital calipers and the tumor volume was calculated using the formula $(\text{length} \times \text{width}^2)/2$. Water was available *ad libitum* and both water and standard laboratory chow was provided, changed and monitored daily. Pair feeding was achieved by monitoring the food intake of the untreated group each 24 h and then providing the pair-fed group with that amount of food for the following 24 h period. All antibodies administered to mice were purified in sterile, endotoxin free PBS. Isotype control IgG2b, isotype control IgG1 and ITEM1 were obtained from Biolegend.

For MEF-Fn14 tumor studies, 11-12 weeks-old female C57BL/6 mice were used and for the C-26 studies, 11-12 weeks-old male CD2F1 (Balb/c x DBA) mice were used and 12-13 weeks-old male mice for the LLC tumor studies. 8-32 weeks-old female and male Fn14 *-/-* mice and 12-21 weeks-old female and male TWEAK *-/-* mice were used (along side age matched control C57Bl/7 mice). Mice received a subcutaneous (s/c) injection of PBS alone or PBS containing 5×10^5 - 5×10^6 cells on day 1 of the experiment using an insulin syringe. Cell lines included mouse embryonic fibroblasts stably infected with human Fn14 (MEF v12 Hras Fn14), an equivalent Fn14-GPI (MEF v12 Hras Fn14-GPI) or the untransfected MEF H-Ras V12 cells (MEF v12 Hras), mouse C-26 or mouse LLC. For antibody treatment experiments, mice were treated by IP injection of 0-10 mg/kg purified antibody in 100 μ l of PBS on the days indicated in the figures.

Muscle function analyses

Grip strength test

As described in detail previously (Murphy et al., 2012), whole body strength was assessed on day 21/21 by means of a grip strength meter (Columbus Instruments, Columbus, OH).

Assessment of functional properties of tibialis anterior muscles *in situ*

On day 22 (C-26 study) or day 11 (MEF study), mice were anesthetized with sodium pentobarbitone (Nembutal; 60 mg/kg; Sigma-Aldrich) via IP injection. The methods for assessment of the contractile properties of the mouse tibialis anterior (TA) muscle *in situ* have been described previously (Murphy et al., 2010). After examining the frequency-force relationship and determining peak tetanic force, muscles were subjected to a 4 min intermittent stimulation protocol to induce muscle fatigue. Muscles were maximally stimulated for 1 sec every 4 sec for the duration of the fatigue protocol. Peak tetanic force was assessed at 5 min and 10 min following cessation of the fatiguing stimulation protocol. At the conclusion of the contractile measurements *in situ*, the TA, extensor digitorum longus (EDL), soleus, plantaris, gastrocnemius and quadriceps muscles as well as the fat (epididymal for C-26 study, subscapular for MEF study) and heart were carefully excised, blotted on filter paper and weighed on an analytical balance. Mice were killed as a consequence of heart excision while still anesthetized deeply.

Skeletal muscle histology

Serial sections (5 μm) were cut transversely through the TA muscle using a refrigerated (-20°C) cryostat (CTI Cryostat; IEC, Needham Heights, MA). Sections were reacted with: laminin (#L9393, Sigma-Aldrich) for determination of mean myofiber cross-sectional area (CSA); succinate dehydrogenase (SDH) to determine activity of oxidative enzymes; and N2.261 (developed by Dr. Helen M. Blau, obtained from the Developmental Studies Hybridoma Bank developed under the auspices of the NICHD and maintained by The University of Iowa, Department of Biology, Iowa City, IA, USA) to assess the percentage of myosin IIa isoforms (Murphy et al., 2010). We have previously shown that mouse TA muscle contains a virtual absence of type I fibers (Murphy et al., 2011) so all non-N2.261 reacting fibers were assumed to represent type IIx/b fibers. Optical density of SDH was determined after 6 min of reactivity for all samples and sections were captured in full color using bright field light microscopy and analysed, as described previously (Murphy et al., 2010). Digital images were obtained using an upright microscope with camera (Axio Imager D1, Carl Zeiss, Wrek, Göttingen, Germany), controlled and quantified by AxioVision AC software (AxioVision AC Rel. 4.7.1, Carl Zeiss).

Real-Time RT-PCR analyses.

Total RNA was extracted from 10-20 mg of TA muscle using a commercially available kit according to the manufacturer's instructions (PureLink RNA Mini Kit, Invitrogen). RNA concentration was determined spectrophotometrically at 260 nm, and the samples stored at -80°C . RNA was transcribed into cDNA using the Invitrogen SuperScriptTM VILO cDNA Synthesis Kit, and the resulting cDNA stored at -20°C for subsequent analysis. Real-Time RT-PCR was performed as described previously (Murphy *et al.*, 2010). Primer sequences for MuRF-1, atrogin-1, IL-6 and TNF- α were as detailed previously (Murphy *et al.*, 2010). The content of single-stranded DNA (ssDNA) in each sample was determined using the Quanti-iT OliGreen ssDNA Assay Kit (Molecular Probes, Eugene, OR), as described previously (Murphy et al., 2010). Gene expression was quantified by normalizing the logarithmic cycle threshold (CT) value ($2^{-\text{CT}}$) to the cDNA content of each sample to obtain the expression $2^{-\text{CT}}/\text{cDNA content}$ ($\text{ng}\cdot\text{ml}^{-1}$).

Activin A model of muscle atrophy

AAV vectors carrying the Activin A expression cassette (or a control AAV, lacking the Activin cDNA) were injected at a dose of 1×10^9 vector genomes into the tibialis anterior (TA) hind-limb muscles of ~ 8 weeks-old male C57BL/6 mice placed under isoflurane anesthesia, as described previously (Chen et al., 2014). Following vector administration and recovery from anesthesia, mice were returned to their home cages, where they were randomly assigned to treatment cohorts receiving repeated administrations of either anti-Fn14 antibody or IgG control antibody. Antibody administration commenced 4 days after injection of vectors, and each mouse received a total of 6 antibody injections prior to the conclusion of experimental endpoint at 4 weeks after vector injection. At the experimental endpoint, the mice were humanely killed via skilled cervical dislocation, and the TA muscles from both hind-limbs were excised to record mass and processed for storage at -80°C .

Supplementary methods

Epitope mapping using bacterially expressed protein

Cloning of hFn14 and mFn14 constructs for bacterial expression

Oligonucleotide primers, engineered with *Nde* I and *Bam* HI restriction sites, were designed, synthesized (Geneworks) and used to amplify the full-length extracellular domain of the human Fn14 (hFn14), the murine Fn14 (mFn14) extracellular domain and the human extracellular domain mutants (R56P, R56A, R56K, R58K) by PCR. Subsequent products were ligated into the vector pGEM-4Z (Promega) cut with *Sma* I. Plasmids from single clone were prepared and inserts were digested from the vector. Restricted inserts were then purified and inserted into pET-15b (Novagen) for expression in *E. coli*.

Expression and purification of (His)₆- proteins

pET-15b derived vectors were transformed into Shuffle T7 Express *E. coli* (New England BioLabs). Expression was induced by 1 mM IPTG at 30 °C for 4 h. Bacterial lysate was loaded onto a 1 ml Ni²⁺-nitrilotriacetic acid (Ni²⁺-NTA)-agarose (Qiagen) column equilibrated with lysis buffer (20 mM Tris-HCl pH 7.8, 300 mM NaCl, 20% (v/v) glycerol, 18 mM imidazole, 1 mM PMSF, Boehringer complete protease inhibitors). The column was first washed with 20 ml of lysis buffer and recombinant proteins were eluted by 300 mM imidazole. Recombinant proteins were dialyzed and concentrated to 1 mg/ml in 25 mM HEPES-KOH (pH 7.4), 100 mM NaCl by a Centricon Centrifugal Filter Devices YM-10 (Millipore).

Gel Filtration Chromatography

(His)₆- proteins were size-fractionated by gel filtration. Protein samples (1 ml) were loaded onto a HiLoad 16/60 Superdex 75 pg column (GE Healthcare) equilibrated with 25 mM HEPES-KOH pH 7.4, 100 mM NaCl at room temperature and were chromatographed at a flow rate of 1.5 ml/min on an ÄKTAexpress system (GE Healthcare). Elution profiles were detected at 280 nm and 1.5 ml fraction were collected.

ELISA screening of monoclonal antibodies with purified (His)₆- proteins

The wells of Maxisorp immunoplates (Nunc) were coated overnight at 4 °C with 2-fold serial dilutions of purified histidine tagged proteins (0.5 µg/ml to 4 ng/ml). Nonspecific protein binding sites were blocked with 1% milk protein in phosphate-buffered saline (PBS) for 1 h at room temperature. Plates were washed with PBST (PBS [10 mM Na-phosphate and 150 mM NaCl], 0.05 % Tween 20). Monoclonal antibodies diluted to 1 µg/ml in PBST (PBS 0.05% Tween 20, pH 7.4) + 0.1% milk protein were added and incubated at room temperature for 2 h in the coated plates. After washing with PBST, a 1:15000 dilution of peroxidase-conjugated AffiniPure goat anti-mouse IgG (H+L) in PBST (Sigma) containing 0.1% milk was added for 1 h at room temperature. ELISAs were developed using TMB substrate and the reaction was stopped using 2 M H₂SO₄ solution. Absorbance at 450 nm was quantified using a Spectramax absorbance spectrophotometer.

Epitope Mapping of Antibodies Using Synthetic Peptides

Peptides representing sub-domains 1 (sub-domain1p), 2 and 3 of hFn14 (Figure S1A) and for the disulfide pair mutant (Cys4&5ΔS; Figure S1F) were synthesized by GLBiochem Ltd. (Shanghai, China) and the cysteine residues for disulfide bonds were chosen as described in the solution structure of the cysteine-rich domain in Fn14 by He *et al.*, (2009). An additional lysine residue was added to the C-terminus in order to attach a biotin moiety and to enable the peptides to bind to neutravidin coated plates (Pre-blocked; Pierce). For these experiments, a control peptide with a biotin at the C-terminus was used as a negative control and isotype control antibodies were also used.

The ELISA was performed essentially according to the manufacturer's recommended protocol (Pierce). Briefly, peptide was coated onto wells (in duplicate) at 1-10 µg/ml for 2 h at room temperature. Wells were washed in PBS/0.05% Tween 20/0.1% BSA 3 times and dilutions of each antibody were added in wash buffer for 1 h with gentle agitation. After another three washes secondary anti-mouse HRP-conjugated (Chemicon) was added at 1/1000 dilution for 1 h shaking. Finally, after 4 further washes the plate was developed using TMB (3,3',5,5'-tetramethylbenzidine) substrate (Pierce), and the reaction was stopped using 2M H₂SO₄ solution. Absorbance at 450 nM was quantified using a Spectromax absorbance spectrophotometer.

Correlation analyses of Fn14 expression with cytokines and survival in TCGA (The Cancer Genome Atlas) human cancers

The mRNA expression and clinical data for stomach, colorectal, lung, head and neck and breast cancers were downloaded from the GDAC (Genome Data Analysis Center) Firehose at the BROAD Institute

(<https://confluence.broadinstitute.org/display/GDAC/Home>).

The expression values are the normalized Log₂ RSEM RNA-Sequencing data (Li *et al.*, 2010). Pearson correlation was calculated for expression of Fn14 with expression of cytokine genes IL-1α, IL-1β, IL-6, IL-8 and TNF. The Benjamini & Hochberg (1995) adjusted P-value was calculated to measure the statistical significance of the observed correlations.

Acknowledgements

We acknowledge financial support from the Cooperative Research Centre for Biomarker Translation and from the Australian National Research Council (NHMRC). We thank Timur Naim, Annabel Chee and Jennifer Trieu (Department of Physiology, The University of Melbourne) for expert technical assistance. We acknowledge the provision of the Activin construct, AAV vectors, and technical assistance by Craig Harrison (Monash Inst of Medical Research / Prince Henry's Inst), Hongwei Qian (Baker IDI), and Justin Chen (Baker IDI and MIMR-PHI). We also acknowledge Stephen Wilcox (at the Ian Potter Centre for Genomics and Personalised Medicine Centre located in the Walter and Eliza Hall Institute for Medical Research) for genome DNA sequencing of the MEF tumour cell lines. John Silke was supported by NHMRC grants #541901, 541902, 602516 and 1025594 and through Victorian State Government Operational Infrastructure Support and Australian Government NHMRC IRIISS (361646). Pascal Schneider is supported by grants from the Swiss National Science Foundation and Nick Hoogenraad, John Silke and Andrew Scott are supported by an NHMRC Development Grant #1075504.

Figure Legends

Figure 1. Antibodies to Fn14 antagonise TWEAK/Fn14 signalling

(A) MEFs transformed with H-Ras V12 and expressing inducible human Fn14 were stained with anti-Fn14 antibodies: 001, 002 or 004, commercial anti-Fn14 antibody (ITEM1) or control non-specific IgG1 and IgG2b. Red histogram traces represent antibody staining. Overlaid black traces indicate staining with secondary antibody alone.

(B) Fn14 antibodies bind specifically to Fn14. Lysates from H-Ras V12 MEFs expressing inducible human Fn14 minus (lane 1) or plus (lane 2) induction were separated on an SDS/PAGE gel, transferred to Nitrocellulose and probed with the indicated purified antibodies.

(C) Fn14 antibodies are specific. HEK293T cells were transiently transfected with the indicated VSV or HA tagged TNF superfamily receptor constructs. 24 h post transfection, cells were harvested, and lysates separated by SDS/PAGE, transferred to PVDF and probed with the Fn14 antibodies 001 or 002 (1 $\mu\text{g/ml}$) anti-VSV or anti-HA antibodies, and detected using an HRP-conjugated secondary antibody. The arrows point to the band corresponding to the expressed protein.

(D) Fn14 antibodies inhibit TWEAK/Fn14-induced signaling. HEK293T cells stably infected with a lentiviral NF- κB GFP reporter were stimulated with or without 100 ng/ml of Fc-TWEAK (pink histograms). Cells were co-incubated with the indicated antibodies 001, 002, 004, control IgG +/- Fc-TWEAK for 24 h. Cells were harvested and GFP fluorescence assessed by flow cytometry (grey histogram).

(E) Fn14 antibodies inhibit TWEAK/Fn14 signaling. Kym1 cells were stimulated with 0, 5, 50 or 200 ng/ml of Fc-TWEAK and 0.1 or 1 $\mu\text{g/ml}$ of purified antibody or 0.05 $\mu\text{g/ml}$ of Fn14-Fc decoy. 24 h later adherent and non-adherent cells were harvested and incubated with Propidium Iodide (PI). Cells were analysed by flow cytometry and the percentage of PI positive cells (% cell death) graphed as mean \pm SEM, n=3.

(F) Fn14 antibodies recognize subdomain 2 of human Fn14 extracellular domain. Sequence representing the extracellular domain of human Fn14 is displayed with the corresponding subdomains 1 and 2 below.

Figure 2. Fn14 inhibition prevents tumor-induced weight loss

(A) The C-26 cell line expresses Fn14 at high levels. Mouse tumor cell lines LLC and C-26 adapted to low serum (0.5% FCS) were harvested and stained using a commercially available anti-Fn14 antibody (ITEM1) followed by an anti-mouse AlexaFluor-647 antibody and analyzed by flow cytometry. Black trace histogram: unstained cells, orange trace; secondary stain only, red trace; anti-Fn14.

(B) The effect of treatment with antibody 002 on C-26 tumor growth. 11 weeks-old CD2F1 male mice were inoculated with 1×10^6 cells s/c in the flank (day 1). As tumors formed, measurements were taken and the tumor volume for each mouse was calculated ($[\text{length} \times \text{width}^2]/2$) and the mean and SEM for C-26 untreated (n=5), C-26 + 002 treated (n=5) plotted. \downarrow : on days 5, 12, 15 and 20 treated mice were injected IP with 002 (10 mg/kg). A drop in average tumor

volume of animals treated at day 21 with antibody 002 coincides with culling of 2 mice due to ethically prescribed limits on tumor size, as indicated in C. * $P < 0.05$ vs. C-26 untreated.

(C) Anti-Fn14 extends survival of mice bearing C-26 tumors. A Kaplan-Meier survival curve for the mice described in panel B. \uparrow : Some 002 treated mice were culled because tumor size reached ethical end-point, however these mice nevertheless retained body weight. $P < 0.01$ log-rank (Mantel-Cox) test.

(D) Anti-Fn14 prevents tumor induced body weight loss. Group averages of mouse weight \pm SEM for the mice described in panel B. Weight at day 1 for each individual mouse = 100%. Weight changes were calculated daily for each mouse and averaged over the total number of mice remaining in each group and SEM was calculated accordingly. \uparrow : Some 002 treated mice culled because tumor size reached ethical end-point. * $P < 0.05$ control vs. C-26 untreated; $\dagger P < 0.05$ control vs. C-26 + 002; $\wedge P < 0.05$ pair-fed vs. C-26 untreated; $\ddagger P < 0.05$ C-26 untreated vs. C-26 + 002.

Figure 3. Fn14 inhibition attenuates muscle wasting and weakness in C-26 tumor-bearing mice.

(A) CD2F1 mice were inoculated with PBS or 0.5×10^6 cells s/c in the flank (day 1). \downarrow : mice were injected IP with control IgG or 002 (10 mg/kg) on days 8, 12 and 16 post inoculation. Body weight was measured daily and standardized to initial starting weight from day 1, and plotted as average group body weight \pm SEM. Relative body mass of untreated C-26 from experiment 1 (grey, n=23) was significantly lower than untreated PBS (blue, n=14) from day 14 ($P < 0.05$). Body mass of untreated C-26 from experiment 2 (white, n=10) was significantly lower than PBS and pair-fed 002 treated C-26 (red, n=10) from days 17 and 16, respectively ($P < 0.05$). Body mass of pair-fed IgG treated C-26 (black, n=10) was significantly lower than PBS and 002 treated C-26 from days 16 and 13, respectively ($P < 0.05$).

(B) Fn14 inhibition significantly attenuates tumor induced weight loss. On day 22 post-inoculation, tumors were surgically excised and weighed and percent change in tumor-free body mass compared to pre-inoculation weight calculated. Data represent means \pm SEM. * $P < 0.05$ vs. PBS; $\dagger P < 0.05$ vs. C-26 from same experiment; $\ddagger P < 0.05$ vs. C-26 + IgG. Cross hatch (//) denotes that the data was obtained in two separate experiments.

(C) Fn14 inhibition treatment prevents loss of muscle mass in tumor bearing mice. On day 22, selected hind limb muscles were excised and weighed. EDL; extensor digitorum longus, Plant; plantaris. Data are means \pm SEM. * $P < 0.05$ vs. PBS; $\dagger P < 0.05$ vs. C-26 from same experiment; $\ddagger P < 0.05$ vs. C-26 + IgG. Cross hatch (//) denotes that the data was obtained in two separate experiments.

(D) Fn14 inhibition treatment prevents loss of muscle mass in tumor bearing mice. On day 22, hearts and selected hind limb muscles were weighed. TA; tibialis anterior, Gastroc; gastrocnemius, Quad; quadriceps. Data are means \pm SEM. * $P < 0.05$ vs. PBS; $\dagger P < 0.05$ vs. C-26 from same experiment; $\ddagger P < 0.05$ vs. C-26 + IgG. Cross hatch (//) denotes that the data was obtained in two separate experiments.

(E) Fn14 inhibition prevents loss of adipose tissue. On day 22, epididymal fat was excised and weighed. Data are means \pm SEM. * $P < 0.05$ vs. PBS; $\dagger P < 0.05$ vs. C-26 from same experiment; $\ddagger P < 0.05$ vs. C-26 + IgG. Cross hatch (//) denotes that the data was obtained in two separate experiments.

(F) Fn14 inhibition improves body strength of tumor bearing mice. On day 21, whole body strength was assessed using a grip strength meter. Data are means \pm SEM. * P <0.05 vs. PBS; † P <0.05 vs. C-26 from same experiment; ‡ P <0.05 vs. C-26 + IgG. Cross hatch (//) denotes that the data was obtained in two separate experiments.

(G) Fn14 inhibition increases peak twitch force in tumor bearing mice. On day 22, peak twitch force of TA muscle was assessed *in situ*. Data are means \pm SEM. * P <0.05 vs. PBS; † P <0.05 vs. C-26 from same experiment; ‡ P <0.05 vs. C-26 + IgG. Cross hatch (//) denotes that the data was obtained in two separate experiments.

(H) Peak tetanic force is improved in anti-Fn14 treated mice. On day 22, peak tetanic force of TA muscle was assessed *in situ*. Data are means \pm SEM. * P <0.05 vs. PBS; † P <0.05 vs. C-26 from same experiment; ‡ P <0.05 vs. C-26 + IgG. Cross hatch (//) denotes that the data was obtained in two separate experiments.

(I) Tetanic force over a range of stimulation frequencies is improved in anti-Fn14 treated mice. On day 22, tetanic force production at stimulation frequencies of 10-350 Hz was assessed in TA muscles *in situ*. Data are means \pm SEM. Force from untreated C-26 from experiment 1 (grey, n=9) was significantly lower than untreated PBS (blue, n=7) from 30 Hz (P <0.05). Force from untreated C-26 from experiment 2 (white, n=9) was significantly lower than PBS and pair-fed 002 treated C-26 (red, n=10) from 40 Hz and 75 Hz, respectively (P <0.05). Force from pair-fed IgG treated C-26 (black, n=9) was significantly lower than PBS and 002 treated C-26 from 150-300 Hz and 100-200 Hz, respectively (P <0.05).

(J) Tetanic force production during fatiguing stimulation is improved in anti-Fn14 treated mice. Tetanic force production during and following 4 minutes of fatiguing intermittent stimulation was assessed in TA muscles *in situ*. Data are means \pm SEM. Force was lower in untreated C-26 from experiment 1 (grey, n=8) compared to untreated PBS (blue, n=7, P <0.001 group main effect). Force was lower in untreated C-26 from experiment 2 (white, n=8) and pair-fed IgG treated C-26 (black, n=9) compared to PBS (P <0.001 group main effect). Force was higher in pair-fed 002 treated C-26 (red, n=10) compared to untreated C-26 from experiment 2 and IgG treated C-26 (P <0.001 group main effect).

Figure 4. Fn14 inhibition induces muscle fiber hypertrophy but does not alter muscle fiber type composition in C-26 tumor-bearing mice.

(A) Fn14 inhibition prevents tumor-induced decrease in muscle fiber size. CD2F1 mice were inoculated with 0.5×10^6 C-26 cells s/c in the flank (day 1). Mice were injected IP with control IgG or 002 (10 mg/kg) on days 8, 12 and 16. On day 22, TA muscles were excised and frozen for histological analysis. Representative images of muscle cross-sections stained with hematoxylin and eosin (H&E) and higher magnification inset are shown. Representative H&E stained images for PBS controls are also shown. Scale bar = 100 μ m.

(B) Fn14 inhibition increases average muscle fiber size in C-26 tumor bearing mice. Muscle sections stained with anti-laminin (red, top panel, scale bar = 100 μ m) were used to quantify muscle fiber cross-sectional area (CSA, bottom panel). Representative laminin-stained images for PBS controls are also shown for comparative purposes but were not quantified due to imaging occurring on a

separate day. Data are means \pm SEM. * P <0.05 vs. C-26; † P <0.05 vs. C-26 + IgG; n=8.

(C) Representative images of muscle sections from tumor-bearing mice stained with anti-laminin (red), anti-myosin IIa (N2.261, green, type IIa fibers) and for succinate dehydrogenase activity (SDH, blue, fiber oxidative capacity). Scale bar = 100 μ m.

(D) Fn14 inhibition of C-26 tumor-bearing mice increases the size of both fast, oxidative (type IIa) and fast, glycolytic (type IIx/b) fibers but has no effect on their proportions in TA muscles, relative to controls. Laminin and N2.261 staining was used to quantify cross-sectional area (CSA, top panel) and relative proportion (bottom panel) of type IIa and type IIx/b fibers. Data are means \pm SEM. * P <0.05 vs. C-26; † P <0.05 vs. C-26 + IgG; n=8.

(E) Fn14 inhibition does not affect oxidative enzyme capacity. SDH and N2.261 staining was used to quantify the oxidative enzyme capacity of type IIa and type IIx/b fibers as well as average muscle fiber oxidative enzyme capacity. Data are means \pm SEM; n=8.

(F) Fn14 inhibition reduced expression of ubiquitin ligases involved in muscle protein degradation. mRNA of MuRF-1 and atrogin-1 in TA muscles was quantitated and the mean value \pm SEM plotted. * P <0.05 vs. PBS; † P <0.05 vs. C-26; ‡ P <0.05 vs. C-26 + IgG; n=8-9. Cross hatch (//) denotes that the data was obtained in two separate experiments.

(G) Fn14 inhibition reduced expression of the pro-inflammatory cytokines IL-6 and TNF mRNA in TA muscles was quantitated and plotted as mean \pm SEM. * P <0.05 vs. PBS; † P <0.05 vs. C-26; ‡ P <0.05 vs. C-26 + IgG ; n=8-9. Cross hatch (//) denotes that the data was obtained in two separate experiments.

Figure 5. Ectopic Fn14 expression in tumors causes loss of body weight and increases vasculature of tumors

(A) Fn14 expression does not affect tumor volume. Female C57BL/6 mice were injected with 5×10^6 tumor cells on day 1. Tumor measurements were taken and the tumor volume for each mouse was calculated ($[\text{length} \times \text{width}^2]/2$) and the mean \pm SEM of 3 independent experiments plotted (Fn14 n=26, Fn14-GPI n=20, H-Ras n=6).

B) Fn14-positive tumors drive rapid weight loss in mice. The body weight for each mouse (from panel A) was assessed daily and weights standardised against starting weight (100%). The average for each group was calculated and graphed; Fn14 (red; n=26), Fn14-GPI (blue; n=20) and H-Ras V12 tumor-bearing mice (yellow; n=6). Error bars are SEM.

(C) Fn14 expression increases tumor vascularity. Representative images of *in situ* tumors from mice inoculated with Fn14 expressing tumor cells (left panel) or Fn14-GPI expressing tumor cells (right panel). Bottom image shows individual tumors from Fn14 (left) and Fn14-GPI (right) resuspended in 9 ml PBS and disaggregated with DispaseII and collagenase A.

(D) Fn14 expression increases tumor invasive capacity. Mice were sacrificed and the whole body was immediately fixed in 10% Neutral buffered Formalin. Tissue comprising the tumor and surrounding skeletal muscle was paraffin embedded, sections prepared and stained with hematoxylin and eosin. Left: Fn14-expressing tumor and right panel: Fn14-GPI expressing tumor, both taken on day 11. Images at 10 \times magnification (upper panel, scale bar 160 μ m) and 40 \times

magnification (lower panel, scale bar 40 μm). Blue box in 10 \times magnification represents area shown in 40 \times images.

Figure 6. Fn14 inhibition prevents cachexia caused by Fn14 tumors

(A) Fn14 inhibition prevents tumor induced body weight loss. Female 11 week old C57BL/6 mice were inoculated with a single s/c injection of mouse embryonic fibroblasts (MEFs) transduced with Fn14 (H-Ras V12 Fn14) or the parental MEF line (H-Ras V12) on day 1. Mice were given a single IP injection of IgG2b isotype control antibody (H-Ras V12, H-Ras V12 Fn14, n=8/group) or antibody 001 (H-Ras V12 Fn14+001, n=8) on day 6. Body weight was measured daily.

(B) Fn14 inhibition prevents tumor induced body weight loss. On day 11, tumors were surgically excised and weighed allowing calculation of the percentage change in tumor-free body weight compared to pre-inoculation weight. Data are means \pm SEM. * P <0.01 vs. MEF v12 Hras; † P <0.05 vs. MEF v12 Hras Fn14.

(C) Antibody 001 prevents loss of muscle mass. On day 11, selected hind limb muscles were excised and weighed. EDL; extensor digitorum longus, Plant; plantaris, TA; tibialis anterior, Gastroc; gastrocnemius, Quad; quadriceps. Data are means \pm SEM (n=8). * P <0.05 vs. MEF v12 Hras; † P <0.05 vs. MEF v12 Hras Fn14.

(D) Effect of antibody 001 on tumor induced loss of heart mass. On day 11, the heart from each mouse was excised and weighed. Data are means \pm SEM (n=8).

(E) Antibody 001 prevents tumor-induced loss of fat mass. On day 11, subscapular fat was excised and weighed. Data are means \pm SEM, n=8. * P <0.05 vs. MEF v12 Hras; † P <0.05 vs. MEF v12 Hras Fn14.

(F) Antibody 001 attenuates the loss of tetanic force over a range of stimulation frequencies (left) but does not alter peak tetanic force (middle) or specific (normalized) force of TA muscles *in situ*. Data are means \pm SEM, n=8. ^a P <0.05 main effect MEF v12 Hras vs. MEF v12 Hras Fn14.

(G) Tetanic force production (expressed relative to initial maximum force) during and after 4 min of fatiguing intermittent stimulation in TA muscles *in situ* is improved in mice treated with antibody 001. Data are means \pm SEM (n=8). ^a P <0.05 main effect MEF v12 Hras vs. MEF v12 Hras Fn14, ^b P <0.05 main effect MEF v12 Hras vs. MEF v12 Hras Fn14+001, ^c P <0.05 main effect MEF v12 Hras Fn14 vs. MEF v12 Hras Fn14+001.

(H) Antibody 001 prevents tumor induced decrease in muscle fiber size. TA muscles were excised and frozen. Representative images of frozen muscle sections stained with H&E, anti-laminin (red), anti-myosin IIa (N2.261, green) and for succinate dehydrogenase activity (SDH, blue) indicating muscle fiber architecture, individual muscle fibers, type IIa fibers and fiber oxidative capacity, respectively. Scale bar = 100 μm .

(I) Laminin stained sections were used to determine average muscle fiber area. Data are means \pm SEM, n=8. * P <0.05 vs. MEF v12 Hras; † P <0.05 vs. MEF v12 Hras Fn14.

(J) Treatment of mice with antibody 001 prevents tumor induced reduction in the size of both fast, oxidative (type IIa) and fast, glycolytic (type IIx/b) fibers in TA muscles. Laminin and N2.261 stained sections were used to quantitate fiber area (top panel) and relative proportion (middle panel). SDH stained samples were used to assess the oxidative enzyme capacity of type IIa and type IIx/b fibers

(bottom panel). Data represent mean \pm SEM (n=8). * P <0.05 vs. MEF v12 Hras; † P <0.05 vs. MEF v12 Hras Fn14.

(K) Antibody 001 prevents tumor induced increase in gene expression of the pro-inflammatory cytokine IL-6 in TA muscles. Data are means \pm SEM, n=8. * P <0.05 vs. MEF v12 Hras; † P <0.05 vs. MEF v12 Hras Fn14.

Figure 7. Comparison of anti-cachectic activity of anti-Fn14 antibodies

(A) Not all anti-Fn14 antibodies reverse tumor induced weight loss. Female C57BL/6 mice were injected with MEF H-Ras V12 Fn14 tumor cells on day 1. On day 7, groups of mice (n=6) were given a single IP injection of purified antibody 001, 002, 004 or ITEM1 (5 mg/kg: ↓) or no treatment. Body weight was measured daily and graphed as weight standardised against starting weight as 100. Error bars represent SEM (Groups starting at day 1 as n=6).

(B) Survival of mice from A graphed as a Kaplan-Meier curve.

(C) Tumor measurements were taken and the tumor volume for each mouse was calculated ($[\text{length} \times \text{width}^2]/2$). Error bars \pm SEM.

Figure 8. Host Fn14 and TWEAK are not involved in cachexia.

(A) Groups of wildtype, *Fn14*^{-/-} or *Tweak*^{-/-} mice were injected with MEF H-Ras V12 Fn14 or Fn14-GPI tumor cells on day 1. Even numbers of male and female mice were used except for groups with an odd starting number. Each mouse was monitored for body weight and after euthanasia, tumors were removed and weighed and a final body mass calculated. Starting weight, final weight and final body mass minus tumor mass (BM-TM) are standardized to starting weight (100%). Mice with no tumors are shown as controls.

(B) Group data for combined males and females for final body mass and tumor-free body mass standardized to starting weight (100%) from mice in panel 8A. * P <0.05 vs. non tumor for that strain; † P <0.05 vs. Fn14 tumor for that strain.

(C) Muscle (TA and Quadriceps, heart) weight was assessed in all mice and epididymal fat was assessed in male mice. Tissue mass was standardized against starting body mass and averaged for each group. Error bars represent SEM. * P <0.05 vs. non tumor for that strain; † P <0.05 vs. Fn14 tumor for that strain.

(D) Anti-TWEAK antibody MTW-1 blocks Tweak-induced NF- κ B activation. HEK293T cells stably infected with a lentiviral NF- κ B GFP reporter were stimulated with 0-200 ng/ml of Fc-TWEAK (grey and underlay as blue histogram). Cells were co-incubated with the indicated antibodies MTW-1, Rat IgG control or antibody 002 +/- Fc-TWEAK for 24 h. Cells were harvested and GFP fluorescence assessed by flow cytometry (red histogram).

(E) Antibodies to TWEAK have no effect on cachexia. Female C57BL/6 mice were injected with MEF H-Ras V12 Fn14 tumor cells on day 1. On day 7, groups of mice (n=8) were given a single IP injection of MTW-1 antibody (anti-Tweak, 10 mg/kg), equivalent negative control IgG antibody (Rat control; 10 mg/kg) or antibody 002 (10 mg/kg: ↓) or no treatment. Body weight was measured daily and graphed as weight standardised against starting weight (100%). Error bars represent SEM (n=8).

(F) The magnitude of wasting observed in muscles injected with AAV vectors expressing Activin was not affected by administration of anti-Fn14 antibodies. Absolute mass values for TA muscles injected with Activin-expressing AAV vectors (right TA muscle, RTA), or control vector (left TA muscle, LTA), as

harvested from mice repeatedly administered either anti-Fn14 antibodies 001 and 002 (antibody B and A, respectively) or IgG control antibody (antibody C). (G) Percentage change in the mass of TA muscles injected with Activin-expressing AAV vectors, compared with contralateral muscles receiving control vector, as harvested from mice repeatedly administered either anti-Fn14 antibodies 001 and 002 or IgG control antibody.

Supplementary Figure legends

Supplementary Figure 1. Epitope mapping of anti-Fn14 antibodies.

(A) Anti-Fn14 antibodies bind to Sub-domain 2 of the extracellular domain of Fn14. ELISAs were performed against peptides representing sub-domains 1 and 2 of the human Fn14 extracellular domain, or control peptide. Antibodies 001, 002, 004, commercially available antibody ITEM1, control IgG1 or IgG2b were assessed for binding to each peptide as indicated. Binding was detected using HRP-conjugated anti-mouse IgG and TMB substrate. Optical density at 450 nm was quantified. The IgG1 isotype control was raised against the control peptide and served as a positive control for the assay.

(B) ELISAs assessing the reactivity of human Fn14 (hFn14), mouse Fn14 (mFn14) or hFn14 single point mutants with the anti-Fn14 monoclonal antibodies. Data was obtained at 0.5 µg/ml antibody concentration. The data for all antibodies tested on a single mutant was standardized against the highest reading.

(C) Amino acid sequence alignment for the extracellular domains of human, mouse and rat Fn14. Differences to human Fn14 are underlined in the mouse and rat sequences.

(D) Antibodies 001 and 002 bind efficiently to the human Fn14 H60A mutant. An ELISA was performed to assess binding of antibodies 001, 002, 004, commercial antibodies ITEM1, ITEM4 and control antibody to a recombinant human Fn14 H60A mutant.

(E) Binding of 001, 002 and 004 to human Fn14 H60K mutant is distinct from ITEM4. An ELISA was performed to assess binding of antibodies 001, 002, 004, commercial antibodies ITEM1, ITEM2 and ITEM4 to a recombinant human Fn14 H60K mutant.

(F) Binding of antibodies 001 and 002 is not dependent on the disulfide bond involving residues C57 and C66 in Fn14. A peptide representing subdomain 2 with the 4th and 5th cysteine residues (C57 and C66) mutated to serine residues (Cys4&5ΔS) was used by ELISA to assess binding of 001, 002, 004, ITEM1 and ITEM4.

Supplementary Figure 2. Fn14 treatment reduced tumor growth rate in C-26 tumor-bearing mice.

CD2F1 mice were inoculated with PBS or 0.5×10^6 cells s/c in the flank (day 1). ↓: mice were injected IP with control IgG or 002 (10 mg/kg) on days 8, 12 and 16 post inoculation. Untreated PBS (n=7), untreated C-26 (n=9), pair-fed IgG treated C-26 (n=10) and pair-fed 002 treated C-26 (n=10). Tumor measurements (length and width) were taken daily and the tumor volume was calculated and graphed over time. * $P < 0.05$ vs. C-26; † $P < 0.05$ vs. C-26 + IgG; n=9-10

Supplementary Figure 3. Anti-Fn14 treatment affects tumor growth and body mass in the Lewis Lung Carcinoma (LLC) tumor model. Male C57BL/6 mice were given a single s/c injection of LLC cells or PBS on day 1. ↓: mice were treated with IP injection of: IgG2b isotype control antibody (PBS + IgG and LLC + IgG, n=8/group) or 002 (PBS + 002 and LLC + 002, n=8) on days 7, 14, 21 and 28, and were sacrificed on day 35.

(A) Tumor measurements were taken daily and graphed as group averages. Data are means ± SEM. ^a*P*<0.01 main effect LLC + IgG vs. LLC + 002.

(B) On day 35, the tumor was surgically excised, weighed and group averages calculated and graphed for tumor volume. Data are means ± SEM. **P*<0.03 vs. LLC + IgG.

(C) Body weight for the PBS groups was measured daily and graphed as group average body weight standardised against starting weight (100%). Data are means ± SEM.

(D) Body weight for the LLC groups was measured daily and graphed as group average body weight standardised against starting weight (100%). Data are means ± SEM. ^a*P*<0.01 main effect LLC + IgG vs. LLC + 002.

Supplementary Figure 4. Anti-Fn14 treatment does not decrease tumor size in mice carrying a MEF v12 Hras Fn14 tumor. Female 11 weeks-old C57BL/6 mice were inoculated with a single s/c injection of mouse embryonic fibroblasts (MEFs) transduced with Fn14 (v12 Hras Fn14) or the parental MEF line (v12 Hras) on day 1. Mice were given a single IP injection of IgG2b isotype control antibody (v12 Hras, v12 Hras Fn14, n=8/group) or 001 (v12 Hras Fn14+001, n=8) on day 6. On day 11, the tumor was surgically excised, weighed and group averages calculated and graphed for tumor mass and volume. Data are means ± SEM.

Supplementary Figure 5. Commercially available Fn14 antibody ITEM1 does not inhibit TWEAK/Fn14-induced NF-κB. HEK293T cells stably infected with a lentiviral NF-κB GFP reporter were stimulated with or without Fc-TWEAK 100 ng/ml. Purified antibodies IgG control (top panels; grey histograms), 001 or ITEM1 (100 ng/ml) were co-incubated with TWEAK for 24 hours and the cells harvested and GFP fluorescence assessed by flow cytometry (red histograms, compare to IgG control grey overlay).

Supplementary Figure 6. Effect of antibody treatment on reversal of cachexia.

(A) Anti-Fn14 antibodies 001 and 002 reversed tumor induced weight loss. Female C57BL/6 mice were inoculated on day 1 with MEF tumor cells expressing Fn14 or Fn14-GPI. On day 8 (after initial weight loss), groups of mice (n=3) were given a single IP injection of purified antibody (5 mg/kg: ↓) or no treatment. Body weight was measured daily and graphed as weight standardized against starting weight (100%). Error bars represent SEM (Groups starting at day 1 as n=3).

(B) Survival of mice from A, graphed as a Kaplan-Meier curve.

Supplementary Figure 7. Correlation between expression of Fn14 and cytokine mRNA in various cancer types.

The correlation between transcript levels of Fn14 and (A) IL-1 α , (B) IL-1 β , (C) IL-6, (D) IL-8 and (E) TNF are depicted for Breast (n=988), Head and Neck (n=303), Lung (n=482), Colorectal (n=316) and Stomach (n=273) cancers.

Benjamini & Hochberg (1995) adjusted P-values calculated to measure statistical significance of observed correlations.

(F) Summary of Fn14 correlation with cytokines in different cancer types. Correlation coefficients that are statistical significant at Benjamini & Hochberg (1995) adjusted P-value < 0.05 are highlighted by (*).

References

- Argilés, J.M., Busquets, S., Toledo, M., and Lopez-Soriano, F.J. (2009). The role of cytokines in cancer cachexia. *Curr Opin Support Palliat Care* 3, 263-268.
- Benjamini, Y., and Hochberg, Y. (1995). Controlling the false discovery rate: a practical and powerful approach to multiple testing. *Journal of the Royal Statistical Society Series B*, 289–300.
- Brown, S.A., Hanscom, H.N., Vu, H., Brew, S.A., and Winkles, J.A. (2006). TWEAK binding to the Fn14 cysteine-rich domain depends on charged residues located in both the A1 and D2 modules. *Biochem. J* 397, 297-304.
- Bruera, E. (1997). ABC of palliative care. Anorexia, cachexia, and nutrition. *BMJ* 315, 1219-1222.
- Burkly, L.C., Michaelson, J.S., and Zheng, T.S. (2011). TWEAK/Fn14 pathway: an immunological switch for shaping tissue responses. *Immunol. Rev.* 244, 99-114.
- Campbell, S., Michaelson, J., Burkly, L., and Putterman, C. (2004). The role of TWEAK/Fn14 in the pathogenesis of inflammation and systemic autoimmunity. *Front. Biosci.* 9, 2273-2284.
- Chen, J.L., Walton, K.L., Winbanks, C.E., Murphy, K.T., Thomson, R.E., Makanji, Y., Qian, H., Lynch, G.S., Harrison, C.A., and Gregorevic, P. (2014). Elevated expression of activins promotes muscle wasting and cachexia. *FASEB J* 28, 1711-1723.
- Culp, P.A., Choi, D., Zhang, Y., Yin, J., Seto, P., Ybarra, S.E., Su, M., Sho, M., Steinle, R., Wong, M.H., *et al.* (2010a). Antibodies to TWEAK receptor inhibit human tumor growth through dual mechanisms. *Clin. Cancer Res.* 16, 497-508.
- Dewys, W.D., Begg, C., Lavin, P.T., Band, P.R., Bennett, J.M., Bertino, J.R., Cohen, M.H., Douglass, H.O., Engstrom, P.F., Ezdinli, E.Z., *et al.* (1980). Prognostic Effect of Weight-Loss Prior to Chemotherapy in Cancer-Patients. *Am. J Med.* 69, 491-497.
- Dogra, C., Changotra, H., Mohan, S., and Kumar, A. (2006). Tumor necrosis factor-like weak inducer of apoptosis inhibits skeletal myogenesis through sustained activation of nuclear factor-kappaB and degradation of MyoD protein. *J. Biol. Chem.* 281, 10327-10336.
- Dogra, C., Changotra, H., Wedhas, N., Qin, X., Wergedal, J.E., and Kumar, A. (2007). TNF-related weak inducer of apoptosis (TWEAK) is a potent skeletal muscle-wasting cytokine. *FASEB J* 21, 1857-1869.
- Dvorak, H.F. (1986). Tumors: wounds that do not heal. Similarities between tumor stroma generation and wound healing. *New Engl. J. Med.* 315, 1650-1659.

Feng, S.L., Guo, Y., Factor, V.M., Thorgeirsson, S.S., Bell, D.W., Testa, J.R., Peifley, K.A., and Winkles, J.A. (2000). The Fn14 immediate-early response gene is induced during liver regeneration and highly expressed in both human and murine hepatocellular carcinomas. *Am. J. Pathol.* *156*, 1253-1261.

Galfre, G., and Milstein, C. (1981). Preparation of monoclonal antibodies: strategies and procedures. *Method Enzymol.* *73*, 3-46.

Girgenrath, M., Weng, S., Kostek, C.A., Browning, B., Wang, M., Brown, S.A., Winkles, J.A., Michaelson, J.S., Allaire, N., Schneider, P., *et al.* (2006). TWEAK, via its receptor Fn14, is a novel regulator of mesenchymal progenitor cells and skeletal muscle regeneration. *The EMBO J.* *25*, 5826-5839.

He, F., Dang, W., Saito, K., Watanabe, S., Kobayashi, N., Guntert, P., Kigawa, T., Tanaka, A., Muto, Y., and Yokoyama, S. (2009). Solution structure of the cysteine-rich domain in Fn14, a member of the tumor necrosis factor receptor superfamily. *Prot. Sci.* *18*, 650-656.

Islam-Ali, B.S., and Tisdale, M.J. (2001). Effect of a tumour-produced lipid-mobilizing factor on protein synthesis and degradation. *Br. J. Cancer* *84*, 1648-1655.

Jakubowski, A., Ambrose, C., Parr, M., Lincecum, J.M., Wang, M.Z., Zheng, T.S., Browning, B., Michaelson, J.S., Baetscher, M., Wang, B., *et al.* (2005). TWEAK induces liver progenitor cell proliferation. *J. Clin. Invest.* *115*, 2330-2340.

Kaduka, Y., Takeda, K., Nakayama, M., Kinoshita, K., Yagita, H., and Okumura, K. (2005). TWEAK mediates anti-tumor effect of tumor-infiltrating macrophage. *Biochem. Biophys. Res. Commun.* *331*, 384-390.

Kamata, K., Kamijo, S., Nakajima, A., Koyanagi, A., Kurosawa, H., Yagita, H., and Okumura, K. (2006). Involvement of TNF-like weak inducer of apoptosis in the pathogenesis of collagen-induced arthritis. *J. Immunol.* *177*, 6433-6439.

Karaca, G., Swiderska-Syn, M., Xie, G., Syn, W.K., Kruger, L., Machado, M.V., Garman, K., Choi, S.S., Michelotti, G.A., Burkly, L.C., *et al.* (2014). TWEAK/Fn14 signaling is required for liver regeneration after partial hepatectomy in mice. *PLoS One* *9*, e83987.

Lam, E.T., Eckhardt, S.G., Messersmith, W., Jimeno, A., O'Bryant, C.L., Ramanathan, R.K., Weiss, G.J., Chadha, M., Fulk, M., Yarian, R., *et al.* (2011). Abstract C18: A phase I study of enavatuzumab (PDL192, ABT-361), a first-in-class human monoclonal antibody targeting TWEAK (tumor necrosis factor-like inducer of apoptosis) receptor, in patients (Pts) with advanced solid tumors. *Mol. Cancer Ther.* *10*, Supplement 1.

Lassen, U.N., Meulendijks, D., Siu, L.L., Karanikas, V., Mau-Sorensen, M., Schellens, J.H., Jonker, D.J., Hansen, A.R., Simcox, M.E., Schostack, K.J., *et al.* (2015). A Phase I Monotherapy Study of RG7212, a First-in-Class Monoclonal

Antibody Targeting TWEAK Signaling in Patients with Advanced Cancers. *Clin. Cancer Res.* 21, 258-266.

Laviano, A., Meguid, M.M., Inui, A., Muscaritoli, M., and Rossi-Fanelli, F. (2005). Therapy insight: Cancer anorexia-cachexia syndrome - when all you can eat is yourself. *Nat. Clin. Pract. Oncol.* 2, 158-165.

Li, B., Ruotti, V., Stewart, R.M., Thomson, J.A., and Dewey, C.N. (2010). RNA-Seq gene expression estimation with read mapping uncertainty. *Bioinformatics* 26, 493-500.

Maccio, A., Madeddu, C., and Mantovani, G. (2012). Current pharmacotherapy options for cancer anorexia and cachexia. *Expert Opinion on Pharmacotherapy* 13, 2453-2472.

McDevitt, T.M., Todorov, P.T., Beck, S.A., Khan, S.H., and Tisdale, M.J. (1995). Purification and characterization of a lipid-mobilizing factor associated with cachexia-inducing tumors in mice and humans. *Cancer Res.* 55, 1458-1463.

Mittal, A., Bhatnagar, S., Kumar, A., Lach-Trifilieff, E., Wauters, S., Li, H., Makonchuk, D.Y., and Glass, D.J. (2010a). The TWEAK-Fn14 system is a critical regulator of denervation-induced skeletal muscle atrophy in mice. *J. Cell Biol.* 188, 833-849.

Mittal, A., Bhatnagar, S., Kumar, A., Paul, P.K., and Kuang, S. (2010b). Genetic ablation of TWEAK augments regeneration and post-injury growth of skeletal muscle in mice. *Am. J. Pathol.* 177, 1732-1742.

Murphy, K.T., Chee, A., Gleeson, B.G., Naim, T., Swiderski, K., Koopman, R., and Lynch, G.S. (2011). Antibody-directed myostatin inhibition enhances muscle mass and function in tumor-bearing mice. *Am. J. Physiol.* 301, R716-R726.

Murphy, K.T., Chee, A., Trieu, J., Naim, T., and Lynch, G.S. (2012). Importance of functional and metabolic impairments in the characterization of the C-26 murine model of cancer cachexia. *Dis. Model Mech.* 5, 533-545.

Murphy, K.T., Koopman, R., Naim, T., Leger, B., Trieu, J., Ibebunjo, C., and Lynch, G.S. (2010). Antibody-directed myostatin inhibition in 21-mo-old mice reveals novel roles for myostatin signaling in skeletal muscle structure and function. *FASEB J.* 24, 4433-4442.

Murphy, K.T., and Lynch, G.S. (2009). Update on emerging drugs for cancer cachexia. *Expert Opin. Emerg. Drugs* 14, 619-632.

Muscaritoli, M., Anker, S.D., Argilés, J., Aversa, Z., Bauer, J.M., Biolo, G., Boirie, Y., Bosaeus, I., Cederholm, T., Costelli, P., *et al.* (2010). Consensus definition of sarcopenia, cachexia and pre-cachexia: joint document elaborated by Special Interest Groups (SIG) "cachexia-anorexia in chronic wasting diseases" and "nutrition in geriatrics". *Clin. Nutr.* 29, 154-159.

Nakayama, M., Ishidoh, K., Kojima, Y., Harada, N., Kominami, E., Okumura, K., and Yagita, H. (2003). Fibroblast growth factor-inducible 14 mediates multiple pathways of TWEAK-induced cell death. *J. Immunol.* *170*, 341-348.

Ohnuma, T., and Holland, J.F. (2009). Anorexia and Cachexia. Supportive Care in Cancer Therapy. In, D.S. Ettinger, ed. (Humana Press), pp. 47-86.

Panguluri, S.K., Bhatnagar, S., Kumar, A., McCarthy, J.J., Srivastava, A.K., Cooper, N.G., and Lundy, R.F. (2010). Genomic profiling of messenger RNAs and microRNAs reveals potential mechanisms of TWEAK-induced skeletal muscle wasting in mice. *PLoS One* *5*, e8760.

Pellegrini, M., Willen, L., Perroud, M., Krushinskie, D., Strauch, K., Cuervo, H., Day, E.S., Schneider, P., and Zheng, T.S. (2013). Structure of the extracellular domains of human and *Xenopus* Fn14: implications in the evolution of TWEAK and Fn14 interactions. *FEBS J* *280*, 1818-1829.

Russell, S.T., and Tisdale, M.J. (2005). The role of glucocorticoids in the induction of zinc-alpha2-glycoprotein expression in adipose tissue in cancer cachexia. *Br. J. Cancer* *92*, 876-881.

Salzmann, S., Seher, A., Trebing, J., Weisenberger, D., Rosenthal, A., Siegmund, D., and Wajant, H. (2013). Fibroblast growth factor inducible (Fn14)-specific antibodies concomitantly display signaling pathway-specific agonistic and antagonistic activity. *J. Biol. Chem.* *288*, 13455-13466.

Schneider, P., Schwenzler, R., Haas, E., Muhlenbeck, F., Schubert, G., Scheurich, P., Tschopp, J., and Wajant, H. (1999). TWEAK can induce cell death via endogenous TNF and TNF receptor 1. *Eur. J. Immunol.* *29*, 1785-1792.

Suragani, R.N., Cadena, S.M., Cawley, S.M., Sako, D., Mitchell, D., Li, R., Davies, M.V., Alexander, M.J., Devine, M., Loveday, K.S., *et al.* (2014). Transforming growth factor-beta superfamily ligand trap ACE-536 corrects anemia by promoting late-stage erythropoiesis. *Nat. Med.* *20*, 408-414.

Tajrishi, M.M., Zheng, T.S., Burkly, L.C., and Kumar, A. (2014). The TWEAK-Fn14 pathway: a potent regulator of skeletal muscle biology in health and disease. *Cytokine Growth F. R.* *25*, 215-225.

Tisdale, M.J. (2009). Mechanisms of cancer cachexia. *Physiol. Rev.* *89*, 381-410.

Tisdale, M.J. (2010). Cancer cachexia. *Curr. Opin. Gastroenterol.* *26*, 146-151.

Varfolomeev, E., Blankenship, J.W., Wayson, S.M., Fedorova, A.V., Kayagaki, N., Garg, P., Zobel, K., Dynek, J.N., Elliott, L.O., Wallweber, H.J., *et al.* (2007). IAP antagonists induce autoubiquitination of c-IAPs, NF-kappaB activation, and TNFalpha-dependent apoptosis. *Cell* *131*, 669-681.

Varfolomeev, E., Goncharov, T., Maecker, H., Zobel, K., Komuves, L.G., Deshayes, K., and Vucic, D. (2012). Cellular inhibitors of apoptosis are global

regulators of NF-kappaB and MAPK activation by members of the TNF family of receptors. *Sci. Signal.* 5, ra22.

Vince, J.E., Chau, D., Callus, B., Wong, W.W., Hawkins, C.J., Schneider, P., McKinlay, M., Benetatos, C.A., Condon, S.M., Chunduru, S.K., *et al.* (2008). TWEAK-FN14 signaling induces lysosomal degradation of a cIAP1-TRAF2 complex to sensitize tumor cells to TNFalpha. *J. Cell Biol.* 182, 171-184.

Vince, J.E., and Silke, J. (2006). TWEAK shall inherit the earth. *Cell Death Differ.* 13, 1842-1844.

Vince, J.E., Wong, W.W., Khan, N., Feltham, R., Chau, D., Ahmed, A.U., Benetatos, C.A., Chunduru, S.K., Condon, S.M., McKinlay, M., *et al.* (2007). IAP antagonists target cIAP1 to induce TNFalpha-dependent apoptosis. *Cell* 131, 682-693.

Wallengren, O., Lundholm, K., and Bosaeus, I. (2013). Diagnostic criteria of cancer cachexia: relation to quality of life, exercise capacity and survival in unselected palliative care patients. *Support Care Cancer* 21, 1569-1577.

Walsh, D., Donnelly, S., and Rybicki, L. (2000). The symptoms of advanced cancer: relationship to age, gender, and performance status in 1,000 patients. *Support Care Cancer.* 8, 175-179.

Warren, S. (1932). The immediate cause of death in cancer. *Am. J. Med. Sci.* 184, 610-613.

Wiley, S.R., Cassiano, L., Lofton, T., Davis-Smith, T., Winkles, J.A., Lindner, V., Liu, H., Daniel, T.O., Smith, C.A., and Fanslow, W.C. (2001). A novel TNF receptor family member binds TWEAK and is implicated in angiogenesis. *Immunity* 15, 837-846.

Winkles, J.A. (2008). The TWEAK-Fn14 cytokine-receptor axis: discovery, biology and therapeutic targeting. *Nat. Rev. Drug Discov.* 7, 411-425.

Yin, X., Luistro, L., Zhong, H., Smith, M., Nevins, T., Schostack, K., Hilton, H., Lin, T.A., Truitt, T., Biondi, D., *et al.* (2013). RG7212 anti-TWEAK mAb inhibits tumor growth through inhibition of tumor cell proliferation and survival signaling and by enhancing the host antitumor immune response. *Clin. Cancer Res* 19, 5686-5698.

Zhou, X., Wang, J.L., Lu, J., Song, Y., Kwak, K.S., Jiao, Q., Rosenfeld, R., Chen, Q., Boone, T., Simonet, W.S., *et al.* (2010). Reversal of cancer cachexia and muscle wasting by ActRIIB antagonism leads to prolonged survival. *Cell* 142, 531-543.

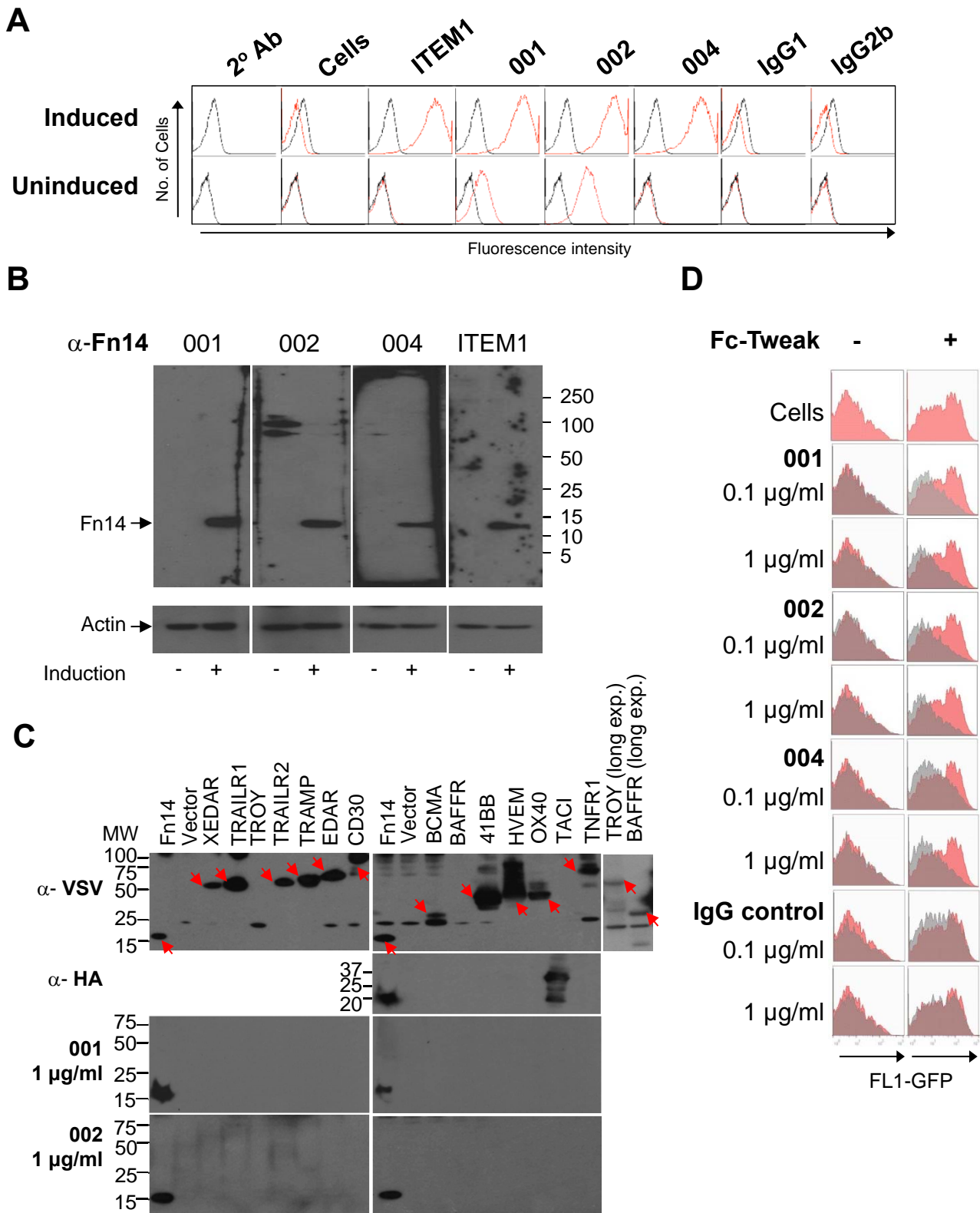


Figure 1

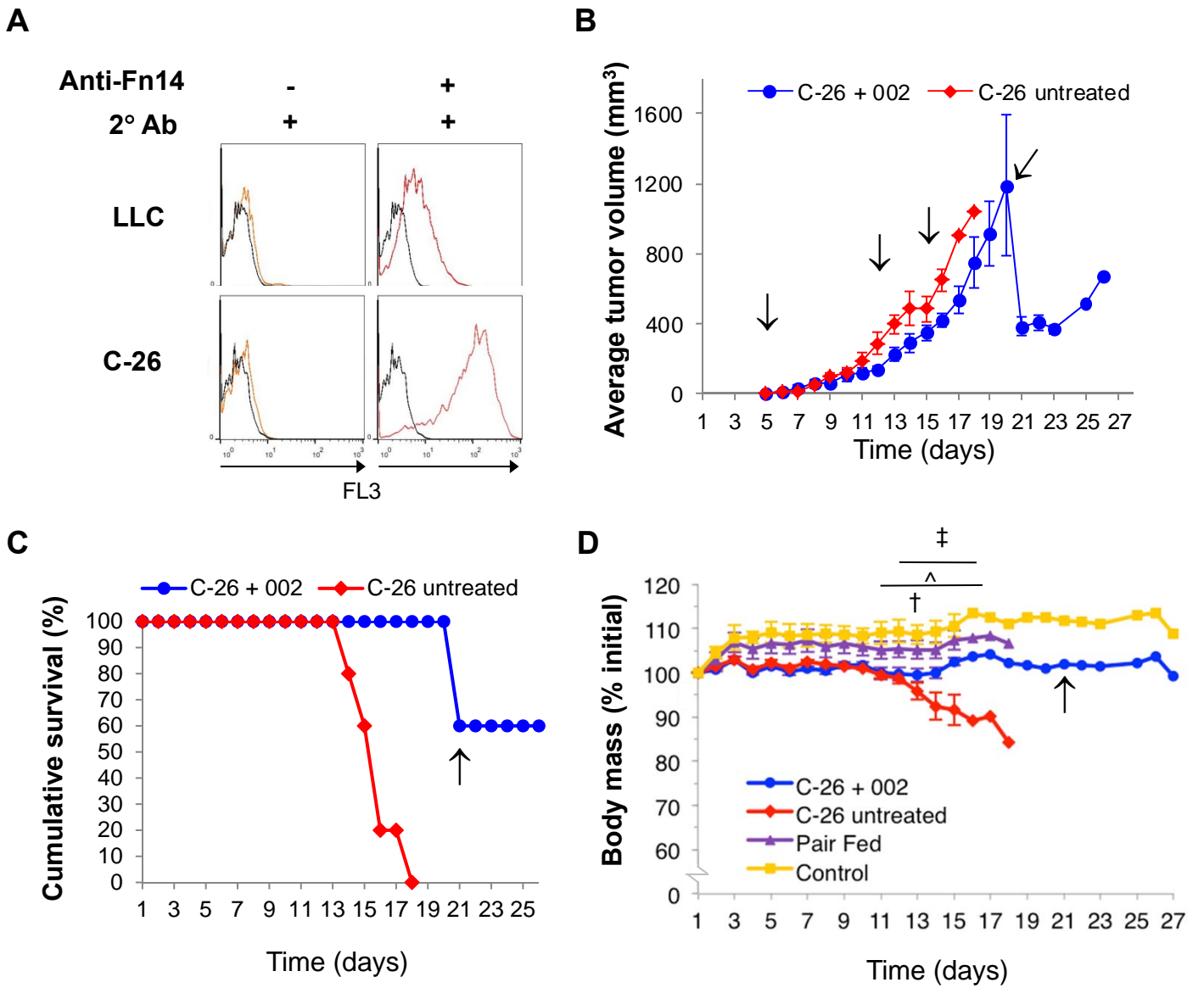


Figure 2

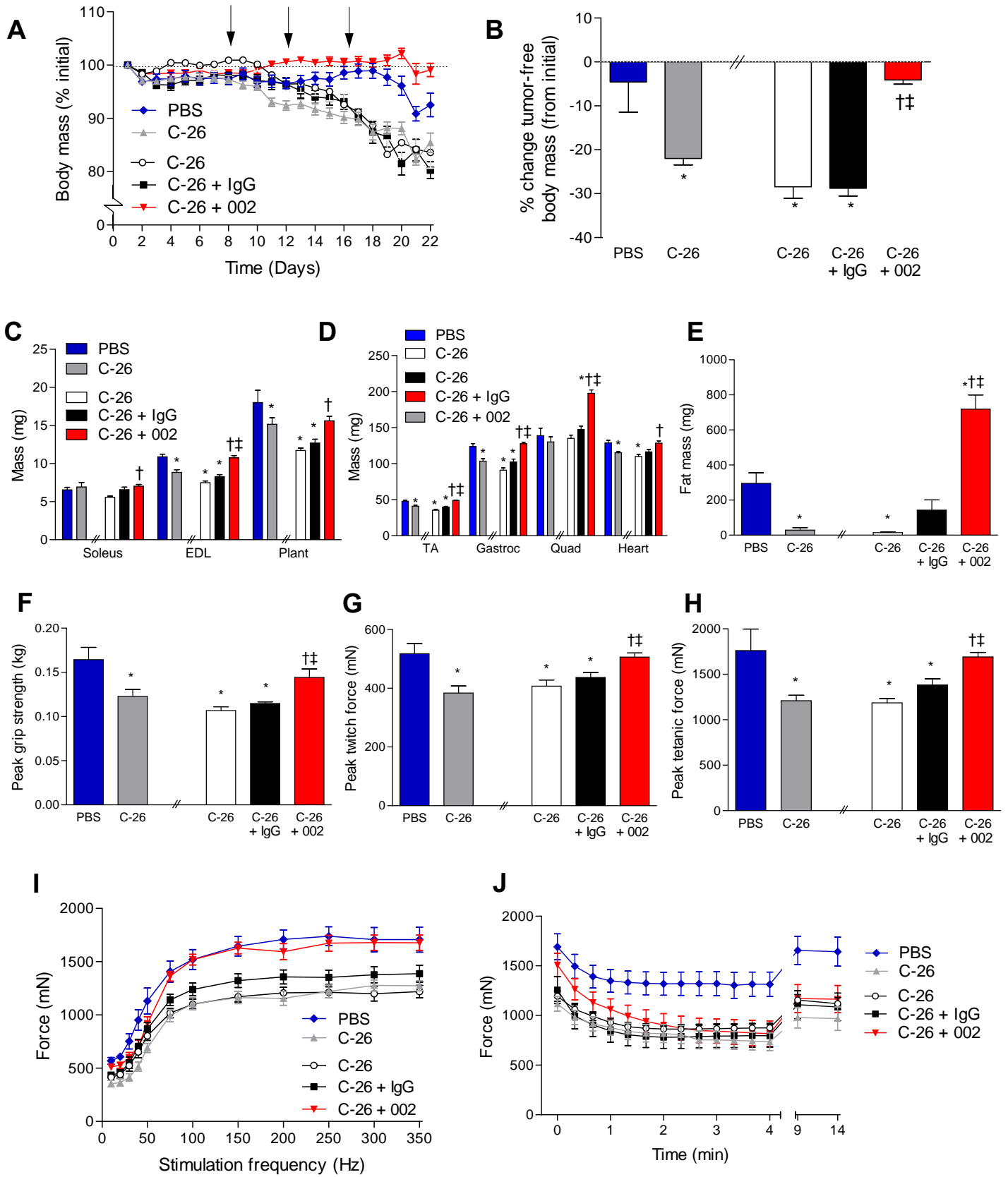


Figure 3

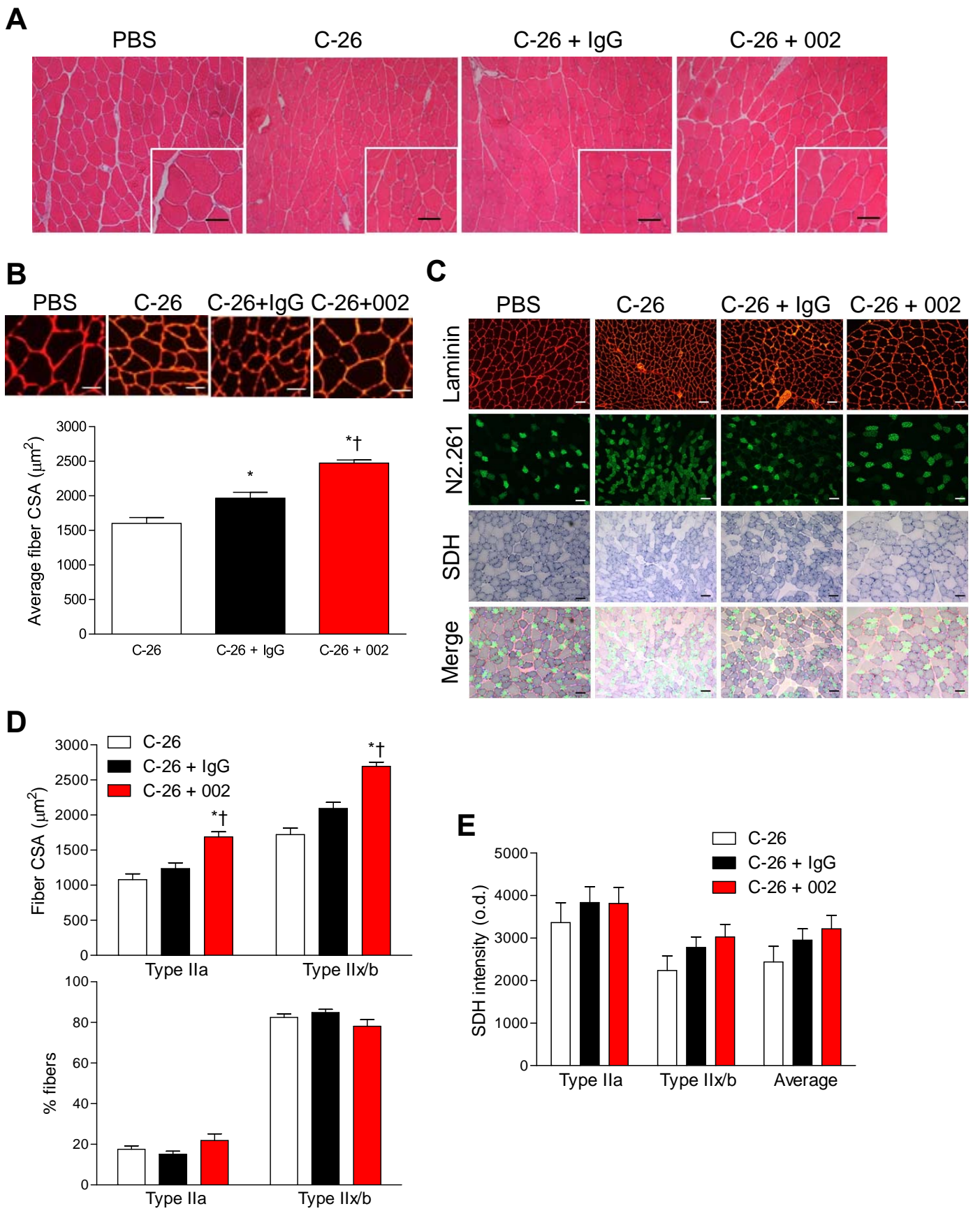
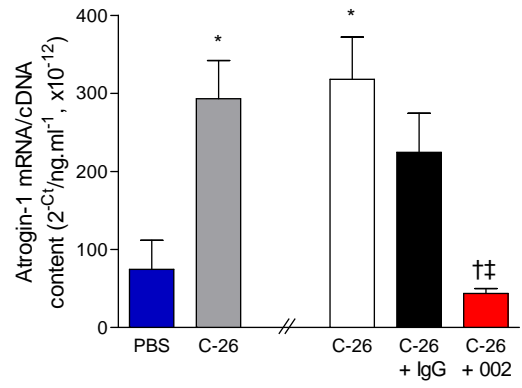
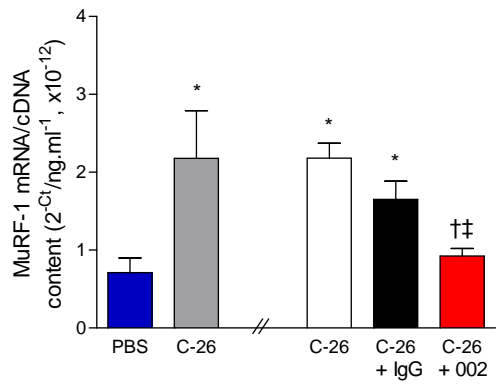
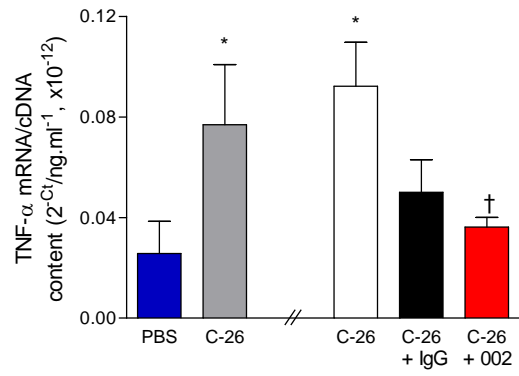
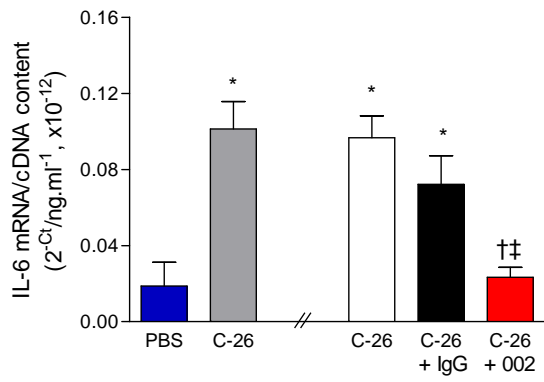


Figure 4

F**G****Figure 4**

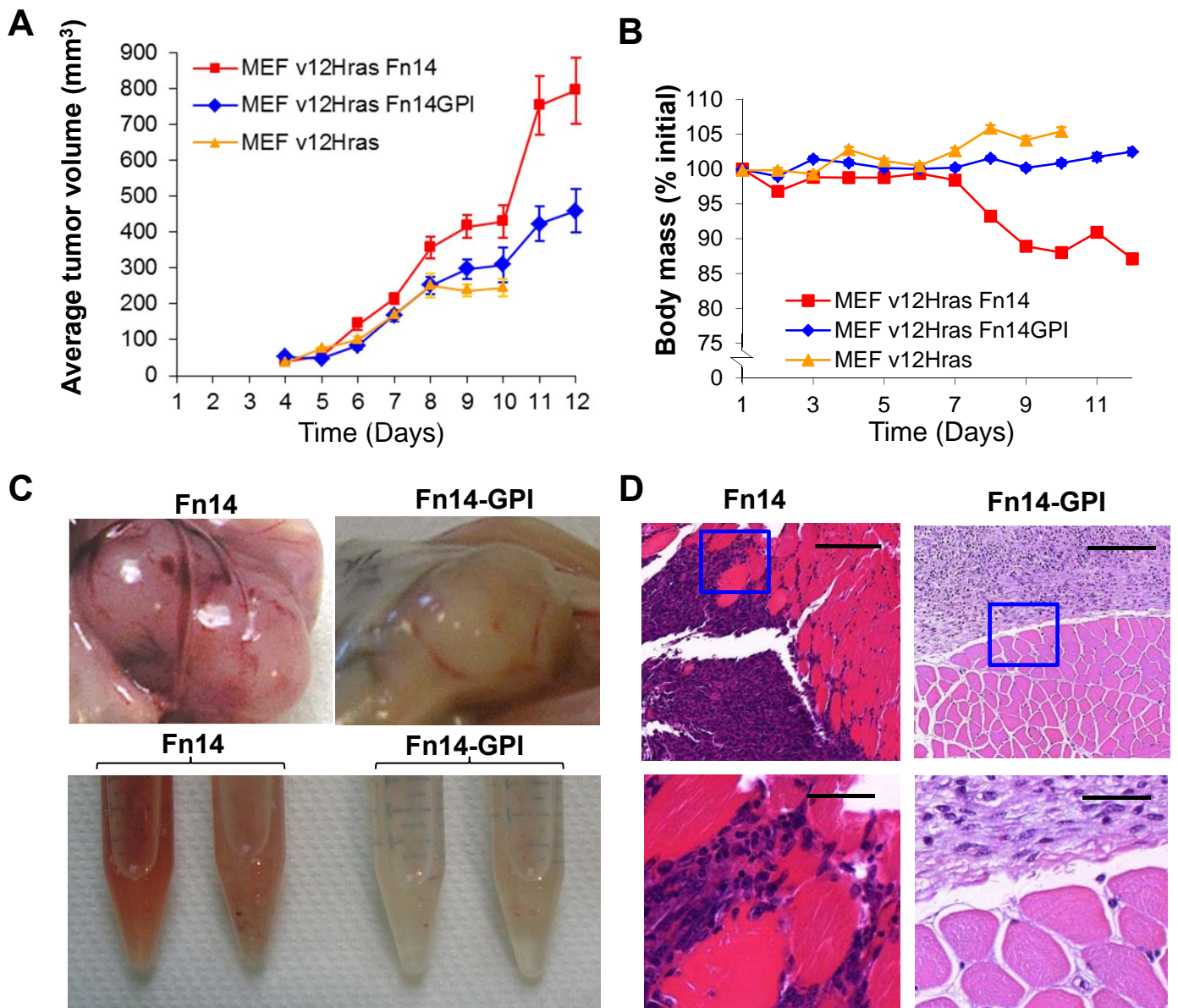


Figure 5

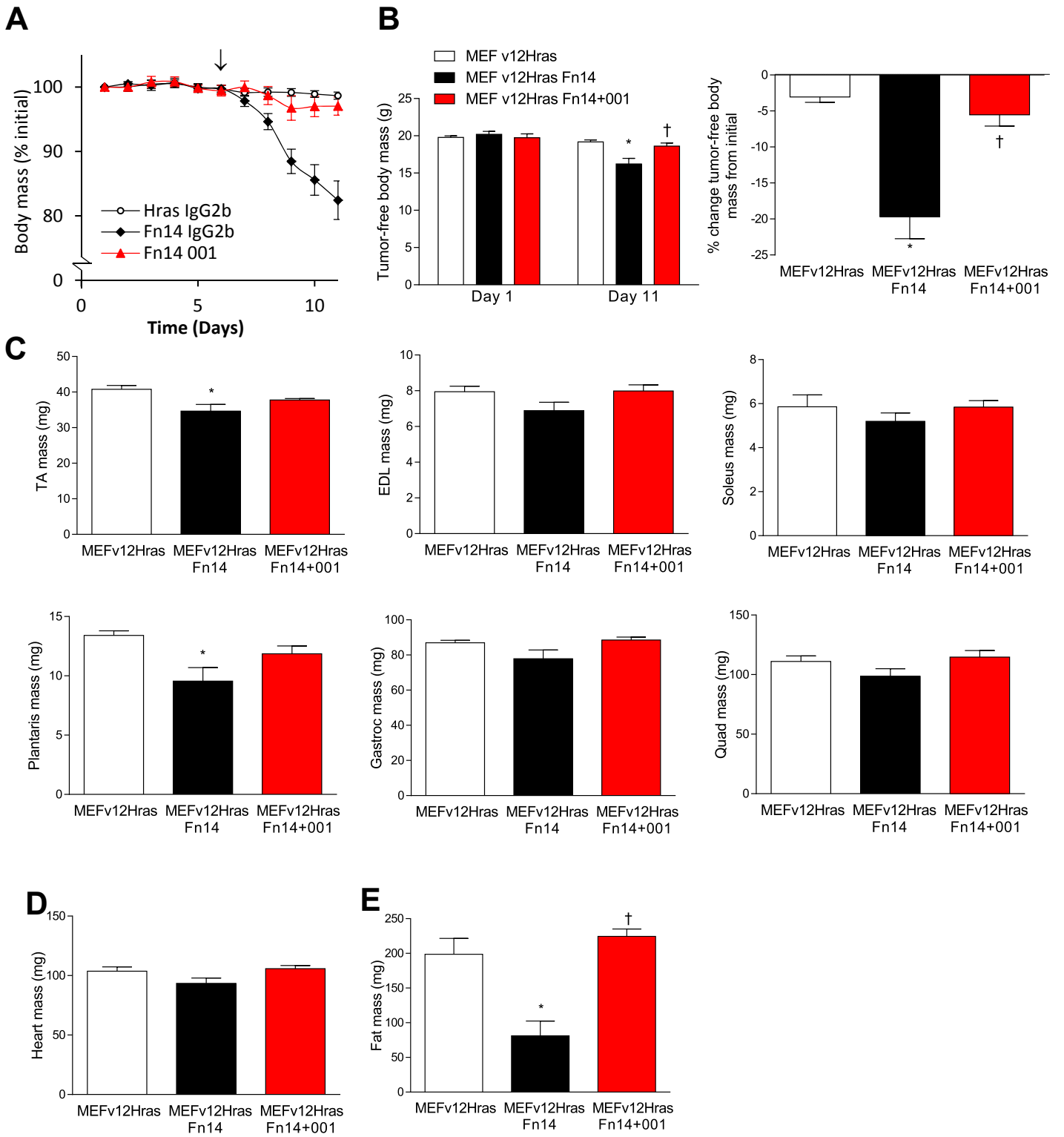


Figure 6

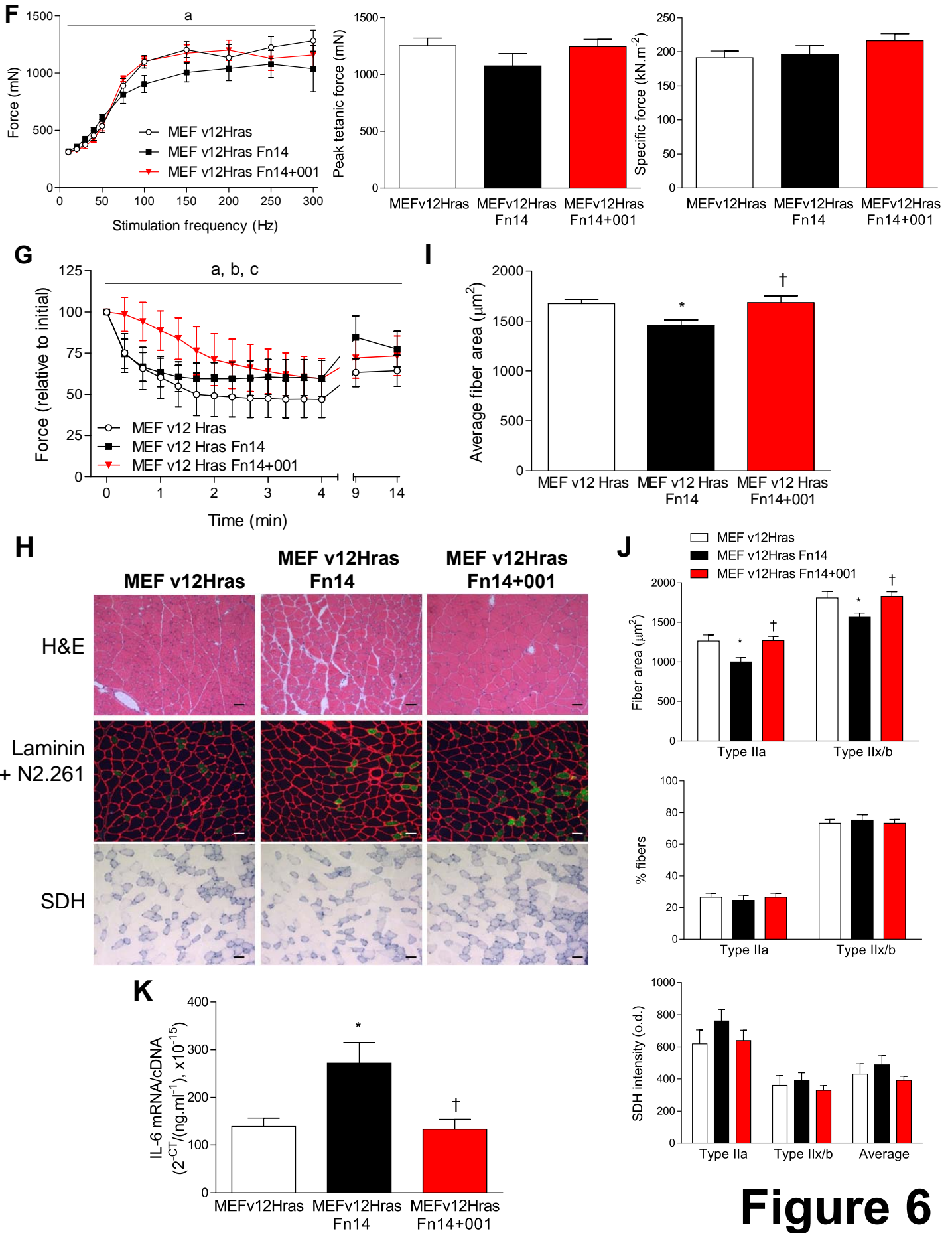


Figure 6

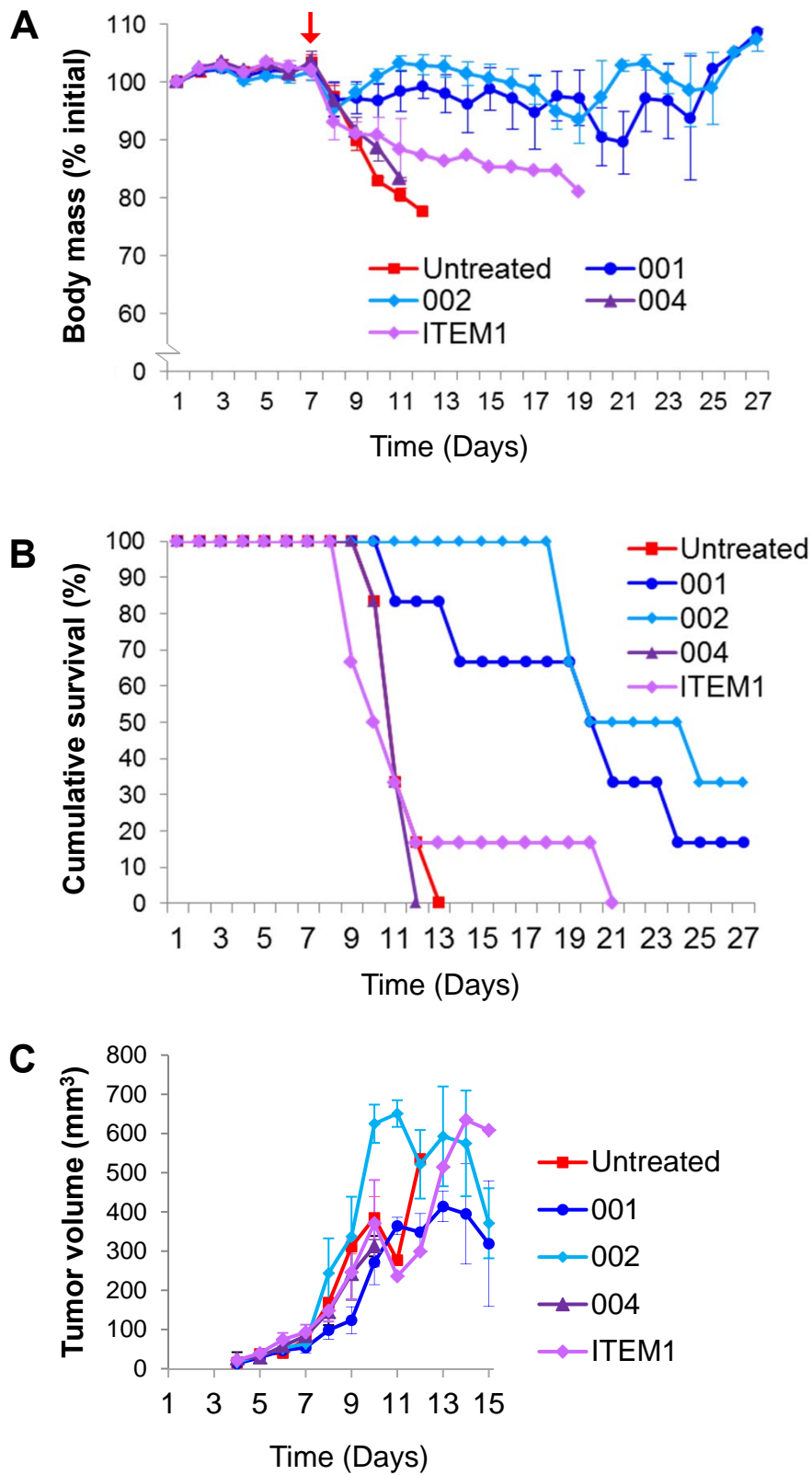


Figure 7

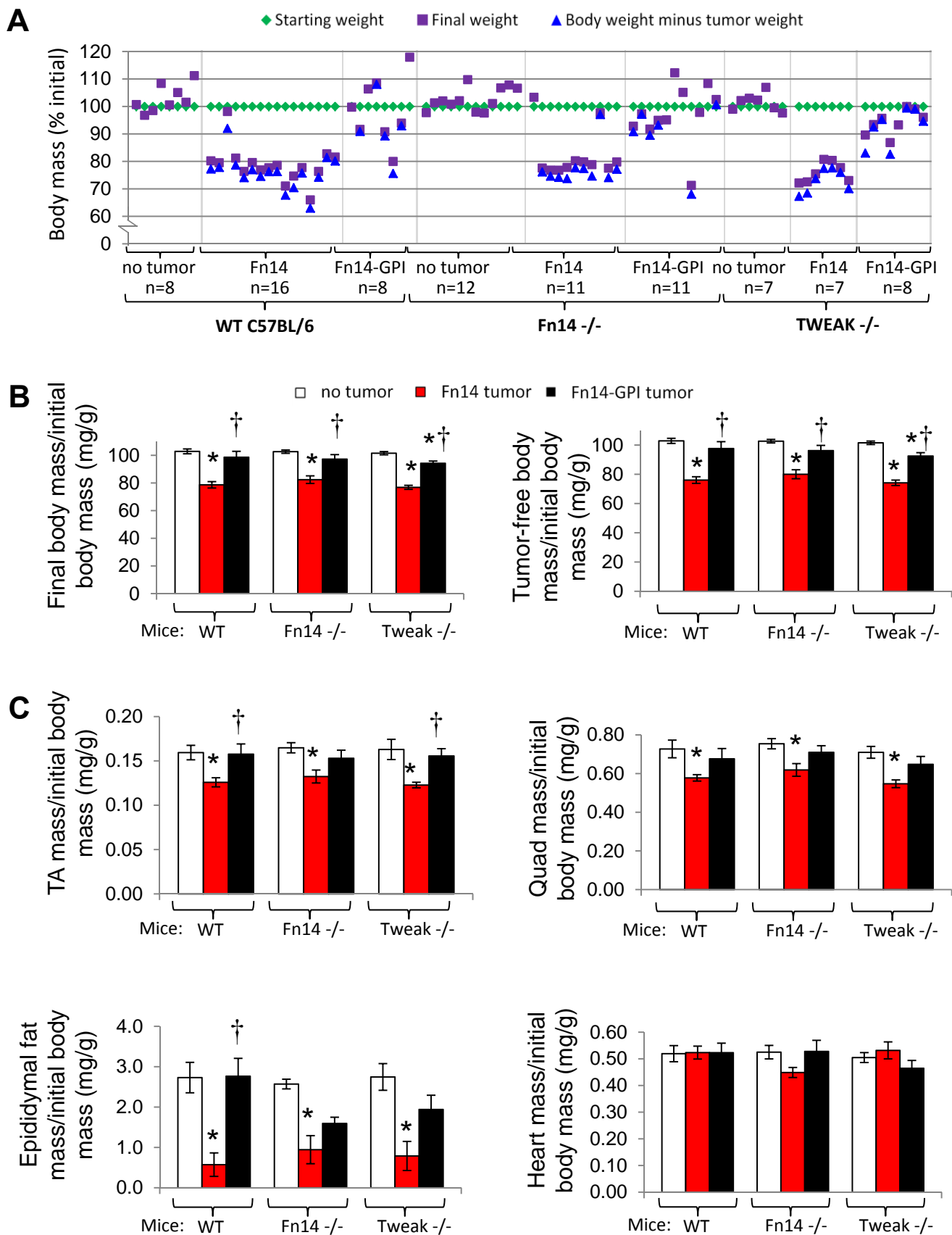


Figure 8

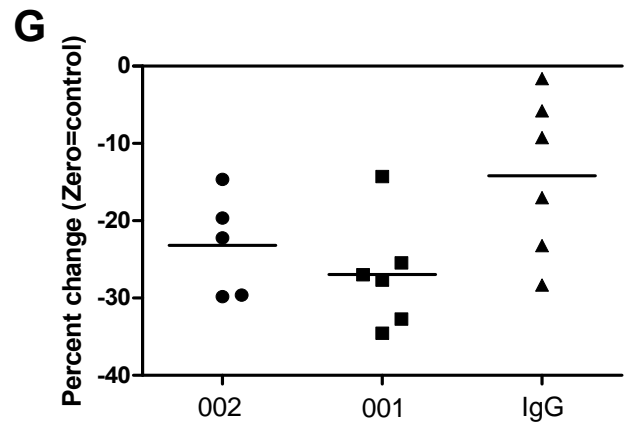
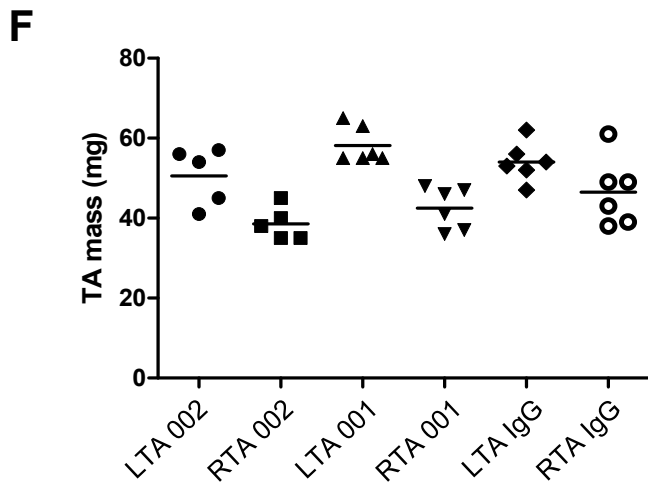
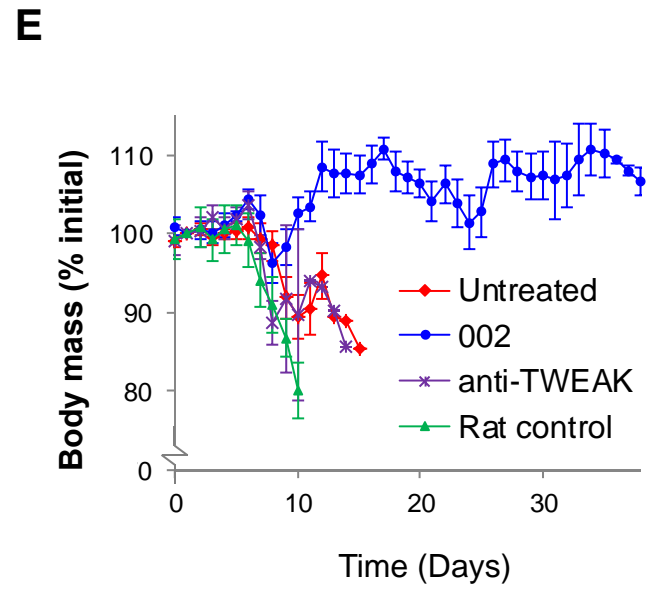
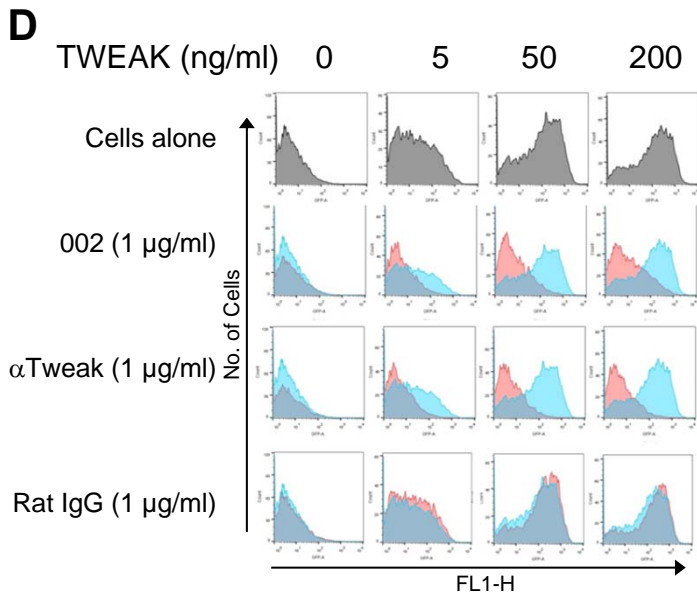


Figure 8

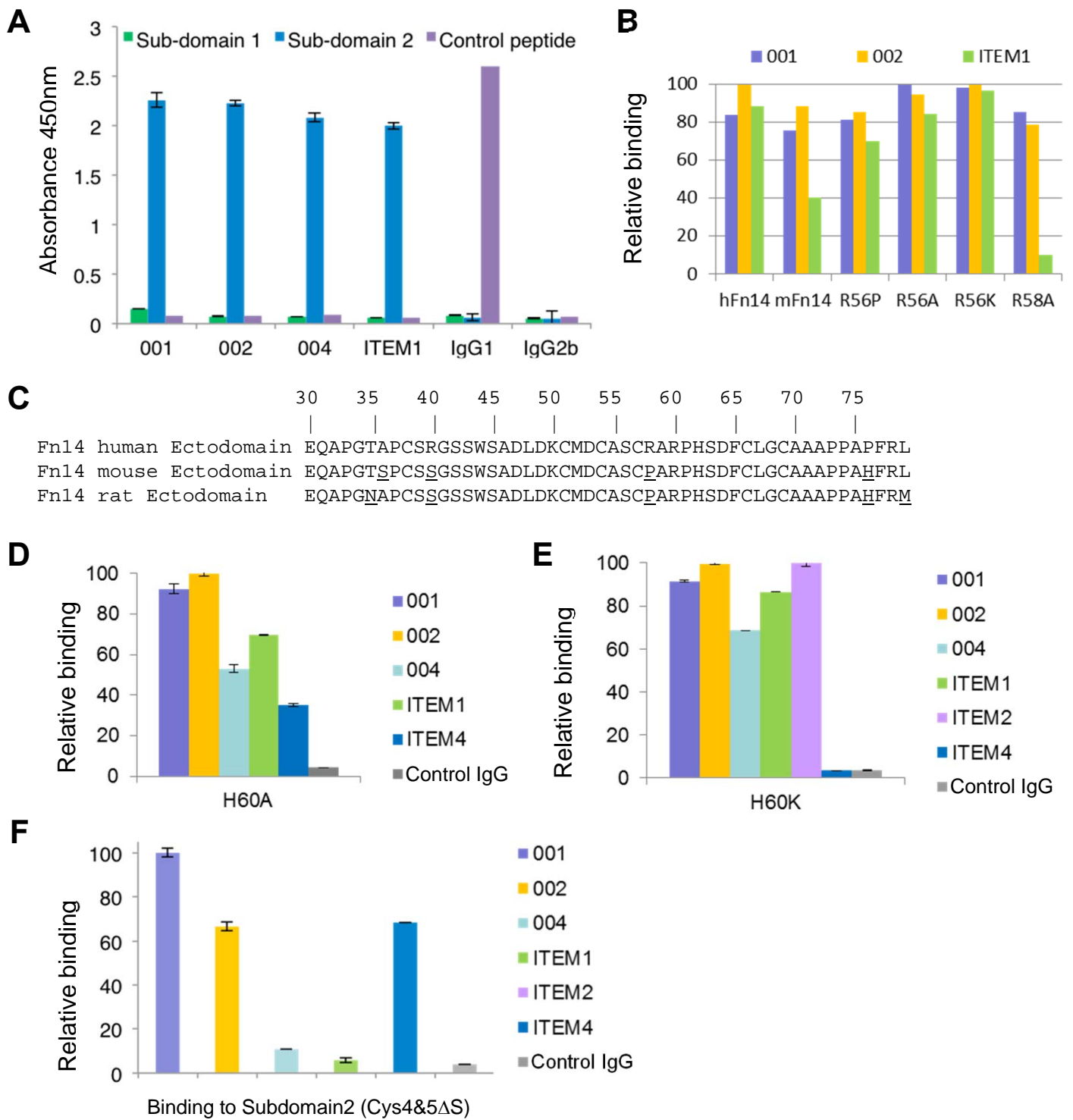


Figure S1

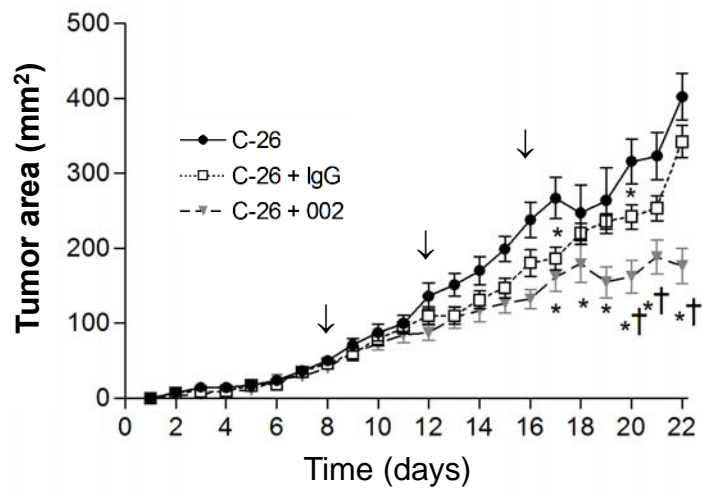


Figure S2

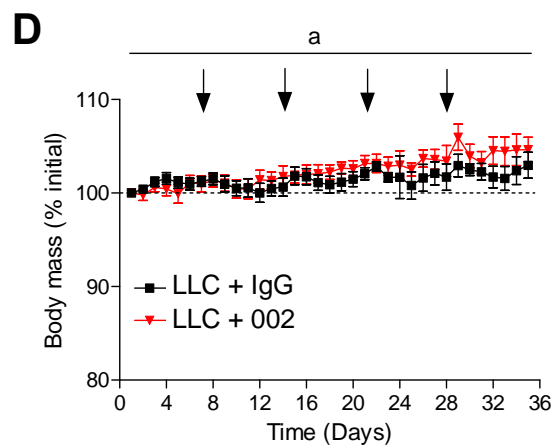
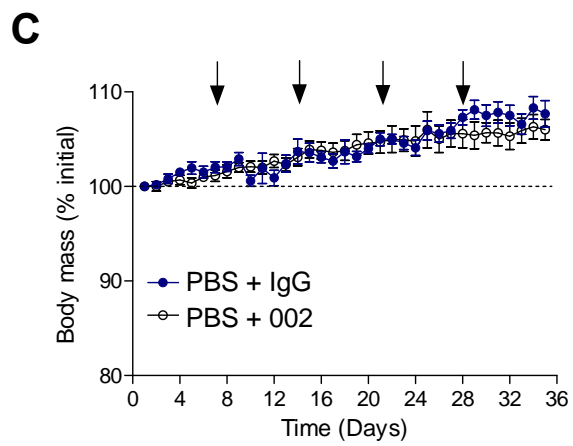
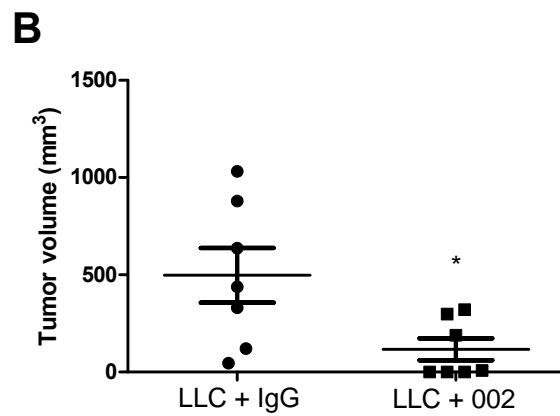
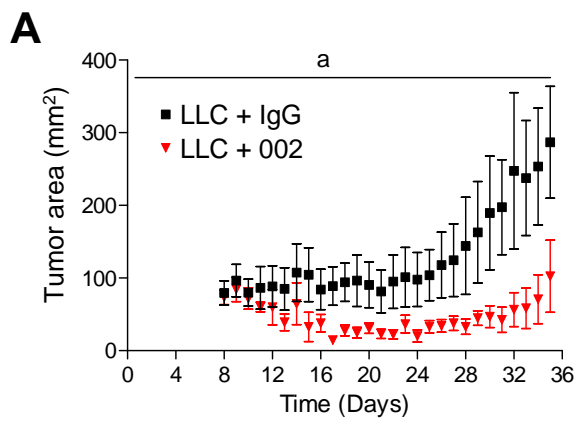


Figure S3

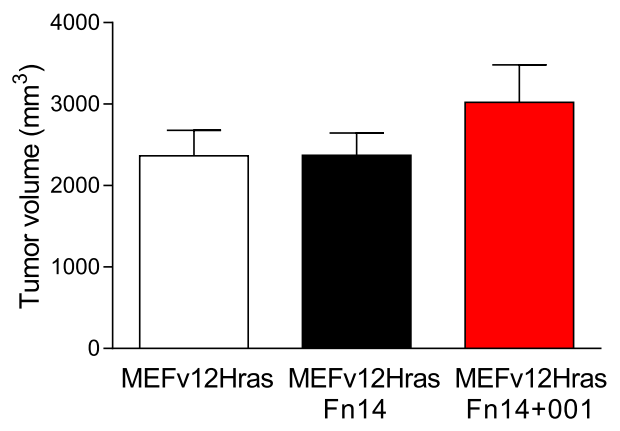
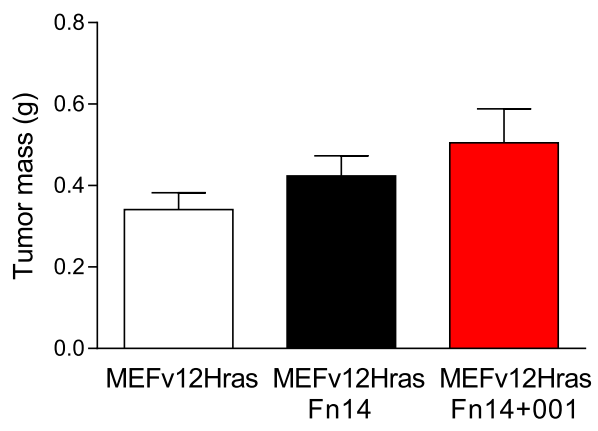


Figure S4

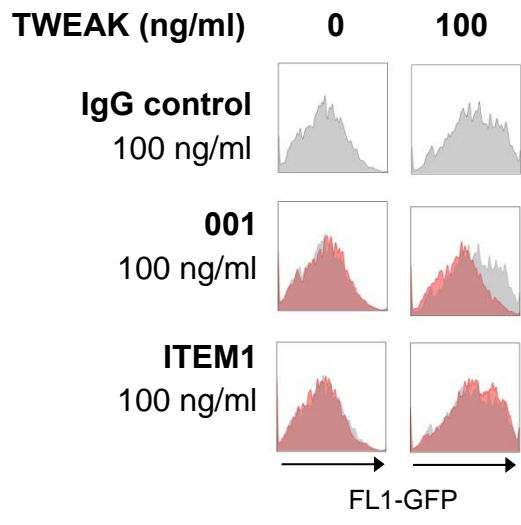


Figure S5

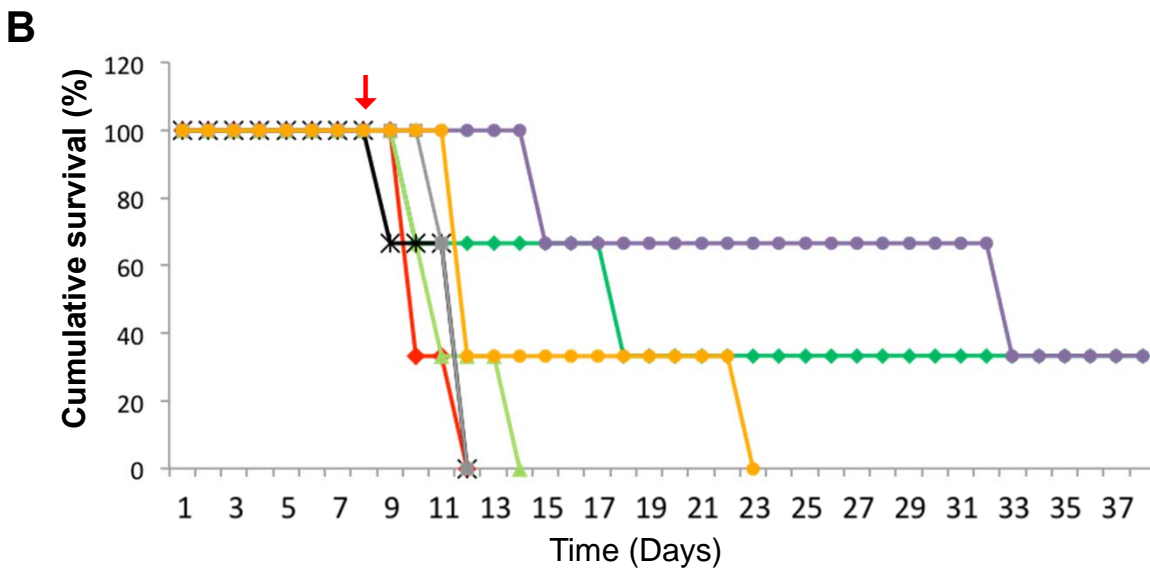
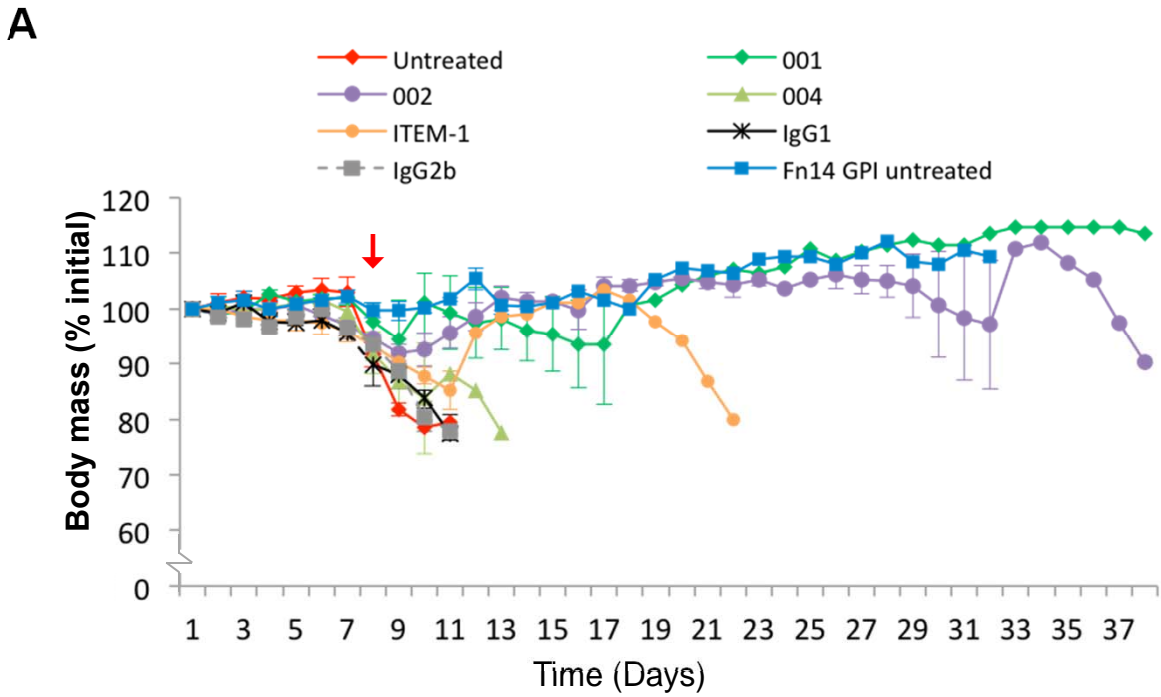
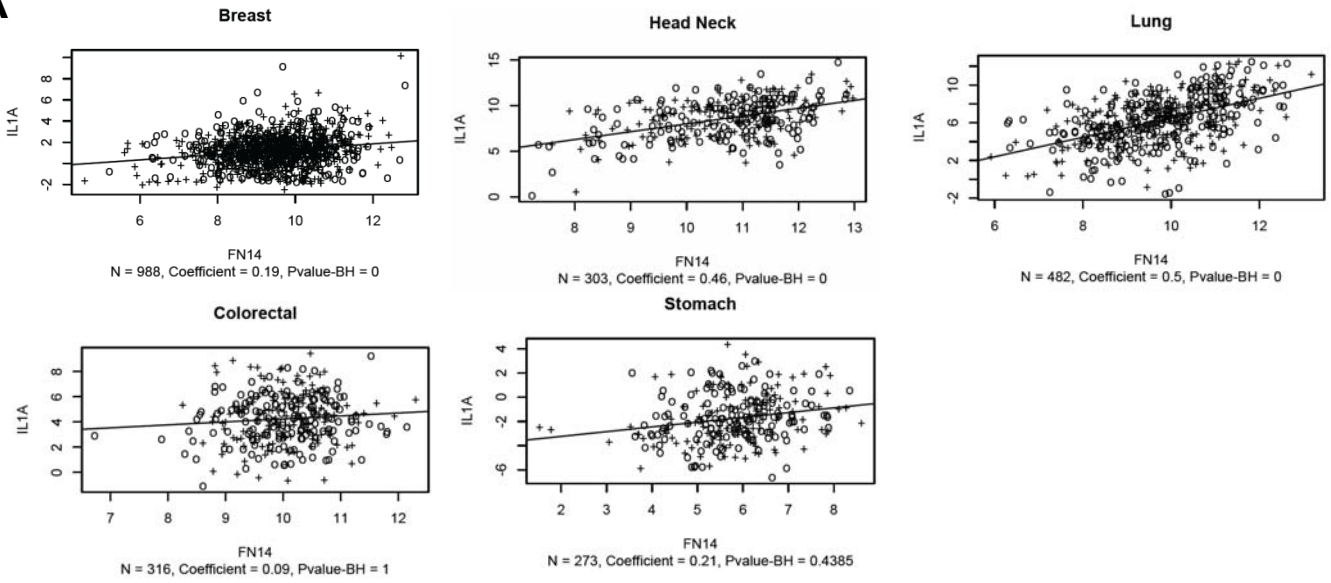
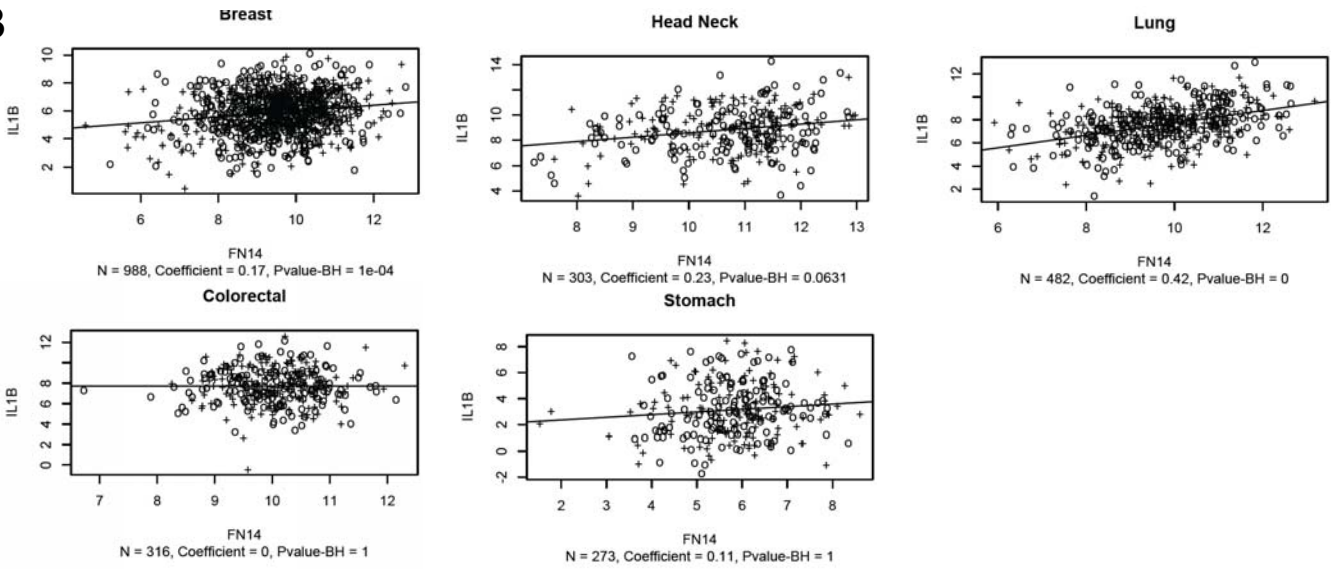
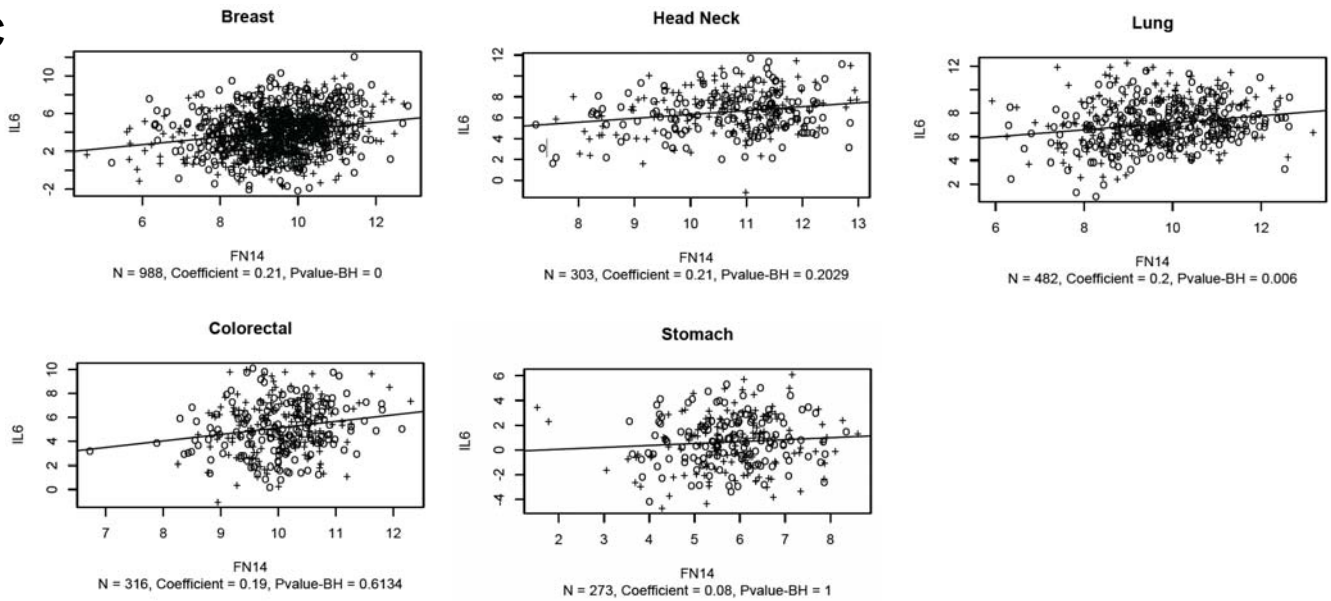
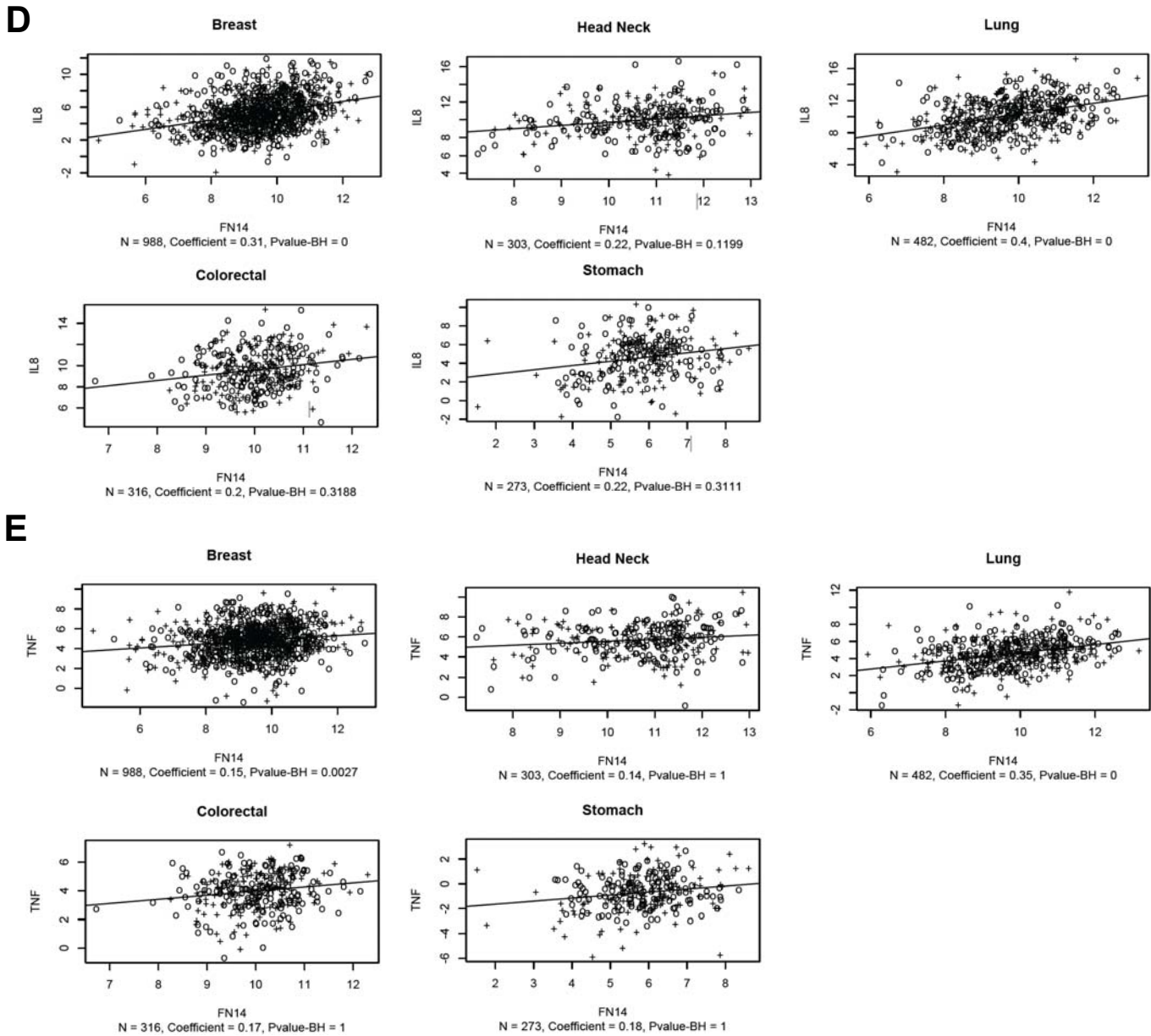


Figure S6

A**B****C****Figure S7**



F

Pearson Correlation Coefficients for expression of Fn14 with cytokines in human cancers

	Breast n=988	Head and Neck n=303	Lung n=482	Colorectal n=316	Stomach n=273
IL-1 α	0.19*	0.46*	0.50*	0.00	0.21
IL-1 β	0.17*	0.23	0.42*	0.09	0.11
IL-6	0.21*	0.21	0.20*	0.19	0.08
IL-8	0.31*	0.22	0.40*	0.20	0.22
TNF	0.15*	0.14	0.35*	0.17	0.18

Figure S7